Optimisation and Performance Evaluation of OFDM Transmission

T.J. Willink, P.J. Vigneron and P.H. Wittke

Terrestrial Wireless Systems

CRC TN No. CRC-TN-98-001
Ottawa, April 1998

CRC Communications Research Centre
Centre de recherches sur les communications

COMMUNICATIONS RESEARCH CENTRE

OPTIMISATION AND PERFORMANCE EVALUATION OF OFDM TRANSMISSION

T.J. Willink, P.J. Vigneron and P.H. Wittke

CRC Technical Note No: 98-001 April 22, 1998

ABSTRACT

In this technical note, the optimisation of OFDM transmission over a linear dispersive channel is considered. The optimum data and power assignments to the subcarriers are derived for both the conventional error probability criterion, and a new criterion based on the normalised mean-square error. The assignments and algorithm hold for channels where performance is degraded by additive noise, intersymbol and interchannel interference. Lower bounds on throughput are derived and are used to compare OFDM performance with conventional single carrier QAM with both linear and decision feedback equalisation. It is shown that OFDM transmission can provide a significant improvement at low and intermediate channel SNRs. The case of a multiuser multicarrier system is considered, in which interference from adjacent users affects the OFDM allocations. A sub-optimal, but more practical, approach to maximising OFDM performance is presented.

RÉSUMÉ

Dans cette note technique, l'optimisation de la transmission en multiplexage orthogonal de division de fréquence (MODF) pour un canal linéaire dispersif est considérée. Les affectations optimales de données et de puissance aux sous-porteuses sont dérivées pour le critère conventionnel de probabilité d'erreur ainsi que pour un nouveau critère basé sur l'erreur normalisée de moyenne au carré. Les affectations et l'algorithme sont valides pour des canaux dégradés par de l'interférence intersymbole et intercanaux ainsi que par l'addition de bruit. Des limites inférieures sur le débit sont derivées et sont utilisées pour comparer la performance du MODF avec la modulation d'amplitude à quadrature (MAQ) conventionnelle à onde porteuse unique utilisant une égalisation de type linéaire ou de type décision à rétroaction. Il est démontré que la transmission MODF peut présenter une amélioration significative pour des canaux à rapport signal sur bruit bas et intermédiaires. Le cas d'un système à utilisateurs multiples et à porteuses multiples est considéré, dans lequel l'interférence des utilisateurs des canaux adjacents affecte les allocations du MODF. Une approche suboptimale, mais un plus pratique, pour maximiser la performance du MODF est présentée.

EXECUTIVE SUMMARY

In order to achieve the maximum benefits from orthogonal frequency division multiplexing (OFDM) or multicarrier transmission, it is necessary to allocate the power and data symbols to the subchannels depending on the respective attenuation and noise characteristics. Subchannels with higher gain-noise ratios are assigned more power and larger signalling constellations.

In this note, the conditions for optimising the assignments of power and data are derived. These conditions are applied to both the traditional criterion, in which an overall bit error probability is specified, and to a new criterion, the normalised mean square error criterion (NMSE). This criterion is based on the ratio of the squared separation of points in the signalling constellation to the mean-square error (MSE) at the system output. It enables a direct comparison of OFDM with single carrier transmission using minimum MSE-based equalisers. For both criteria, the optimal conditions can be achieved using an iterative approach, an example of which is presented here.

Analytic lower bounds on OFDM performance are found for both criteria, and comparisons are made with equalised single carrier transmission. It is found that, using the error probability criterion, OFDM will always perform at least as well as decision feedback equalisation with a single carrier. For the NMSE criterion, the lower bound on OFDM throughput is lower than the upper bound on throughput for the decision feedback equalised single carrier. However, at low SNRs, both bounds are loose, hence it is expected that OFDM will outperform single carrier transmission at low and moderate SNRs, with performance being comparable at high SNRs.

An AWGN channel with a mid-band notch of 15 dB is used to demonstrate the optimal assignments of power and data among the subchannels, using continuously variable numbers of bits per symbol on each subchannel. It is shown that, as predicted, optimal OFDM outperforms equalised single carrier transmission at low and moderate SNRs for both criteria. As the SNR increases, the difference between the two systems decreases. The case of integer bit assignments is also considered, and it is seen again that higher throughput is achieved using OFDM compared to a single carrier.

In the case of multiuser multicarrier systems, the lack of synchronisation between users means that there is inter-channel interference (ICI) between adjacent users on the uplink. Analysis of this interference for a slow fading, frequency selective channel shows that the levels of ICI is dependent on the timing offset. As a first approximation, this ICI can be treated as AWGN on each subchannel, hence the optimisation conditions derived can be applied. An example of a multiuser system demonstrates the effects of the timing offsets on the optimal allocations of power and data.

The conditions derived for optimising OFDM require an iterative solution which can be slow to converge. An empirical relationship between the subchannel gain-noise characteristics and the power and data assignements is derived, which leads to a more easily computed, nearly optimal solution of the OFDM resource allocation problem. This solution uses a modification to the water-pouring approach, associated with Shannon's theory of capacity, to achieve a power assignment that is very close to optimum. The associated data assignment is farther from optimum, but the allocations are much faster to achieve.

CONTENTS

1 INTRODUCTION

Multicarrier transmission, also known as multichannel transmission or orthogonal frequency division multiplexing (OFDM), has seen application in recent years as an approach to the problem of transmitting data over channels which are severely distorted and may suffer from additive or impulsive noise, multipath fading or crosstalk [4, 9, 10, 18, 38].

1.1 GENERAL DESCRIPTION

The principle of OFDM is to divide the channel into narrow subchannels each of which carries a subset of the data. At the transmitter, the data sequence is divided into sub-streams which are used to modulate or key the subcarriers separately. The modulated carriers are summed for transmission over the channel, and are separated again at the receiver. The demodulated signals are then reassembled in their original order. This process is illustrated in Fig. 1.1.

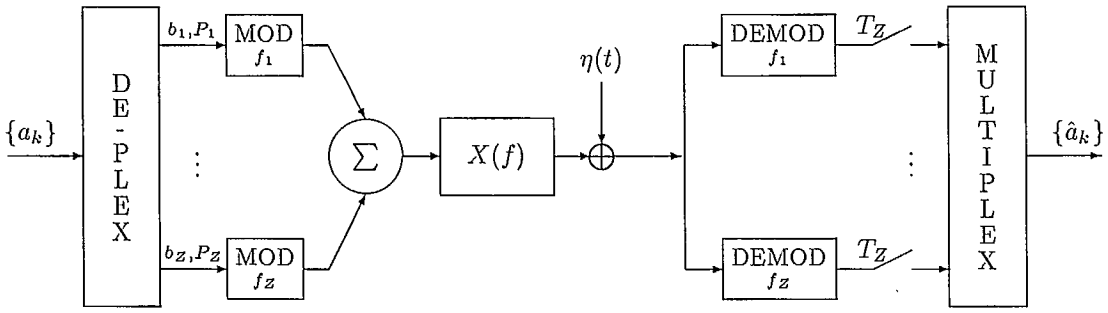

Figure 1.1: Multicarrier system

If each subchannel is sufficiently narrow and interference between adjacent channels is prevented, the system can be considered to be a set of parallel Nyquist I channels. Thus the effects of frequency dependent distortion across the channel bandwidth are limited and the subchannels with the worst gain-to-noise ratios can be used to a lesser extent or avoided altogether. The symbol period on each subchannel is far greater than for the equivalent data rate using a single carrier, thus the effects of impulsive noise and fading are spread over a large number of low bit-rate symbols in parallel, rather than completely destroying a few high bit-rate sequential symbols.

In real applications it may be necessary to mitigate the effects of intersymbol interference (ISI) by introducing a "guard period" between transmitted symbols on each subchannel. If the guard period is at least as long as the subchannel impulse response, then the ISI can be completely eliminated at the cost of a reduction in the data rate.

Interference between adjacent subchannels can be reduced or eliminated with suitable signal design. For example, if the spectrum of each subchannel QAM signal is band-limited to overlap only its immediate neighbours, the sub-streams can be made orthogonal by "staggering" or offsetting the modulations in time. Thus the in-phase signal on subchannel k, for example, is delayed by half a symbol period with respect to the quadrature signal on that subchannel. On the adjacent subchannels, $k-1$ and $k+1$, the quadrature

signals are delayed by half a symbol period with respect to the in-phase signals [3, sec.4.5.3]. This staggering does not affect the spectra of the transmitted signals.

A good introduction to the concepts involved in multicarrier transmission can be found in [4] and [3, sec.4.5].

1.2 A BRIEF HISTORY

Several modems in the 1950's and 60's transmitted high-speed serial data by modulating several low-speed, parallel carriers, including the ANDEFT® /SC-320 [24] and the AN/GSC-10 [37] which both used multicarrier phase shift keying (PSK) to transmit at 4800 bits/s over HF radio channels of bandwidth 3 kHz. The effects of interference caused by ionospheric distortions and sharp cut-off filters were reduced using guard intervals between transmitted symbols. The subcarrier spacing was increased to reduce interchannel interference.

The need for guard intervals in the time and frequency domains was reduced when Chang showed that a wide range of band-limited orthogonal signals could be designed for transmitting amplitude modulated data over parallel subchannels [6, 7]. He specified conditions on the data timing and carrier phases which allowed the signal spectra to overlap the immediately adjacent sub-bands, thereby eliminating the need for filters with sharp cut-offs. Saltzberg [30] considered multicarrier QAM transmission in which the overlapping signal spectra met Chang's criteria for orthogonality. Interchannel interference was eliminated for a distortionless channel by staggering the timing on adjacent subchannels such that they were in phase quadrature.

More recently, multicarrier modulation has been tried for a variety of applications, for example, the digital subscriber line (1.6 Mbps over the twisted copper pair) [8, 9], the groupband (60–108 kHz) [16], digital radio broadcasting [20, 22], cellular mobile [11] and mobile FM radio [5]. For a more detailed literature review, see [33].

1.3 VARIABLE ALLOCATION OF RESOURCES

Trellis coding was used in [28] to increase the coding gain of the overall system at the cost of an increase in complexity at the receiver where a Viterbi decoder was implemented. To counteract the effects of nulls in the channel response, for example those caused by channel transformers that do not pass dc, the data rate was varied across the channel, and the power was allocated according to the "water-pouring" analogy [14, sec.8.3].

Kalet also considered the variable allocation of data and transmission power in [17] and [18]. He optimised the system to achieve maximum data throughput for a given transmission power and overall error probability, based on the assumption that each subchannel must achieve the same overall symbol error rate. In [4], Bingham suggested the alternate condition for optimality that the bit error rates must be equal across the subchannels used.

No rigorous or mathematical justification has been given for the assumption that each subchannel must achieve the same performance standard. In [13], it was called the "no weak link" principle, which suggests that the authors believed that allowing some subchannels to operate below the standard while others achieved a superior performance would cause the overall system to be substantially degraded. However, intuitively one would expect situations where not all subchannels would be able to meet the given standard.

Kalet [18] concluded that multicarrier transmission can demonstrate an appreciable improvement only when a deep null exists in the transmission channel. In [36], Zervos and Kalet applied the multicarrier data and power assignments based on equal symbol error rates from [18] to the twisted copper pair channel. They found that the difference in performance between the multicarrier and optimised single carrier using a zero-forcing decision feedback equaliser was negligible. Feig [12] used an equal bit error criterion across the subchannels of a magnetic recording channel model, and quantised the data rates on each to fit one of a set of signalling constellations. This resulted in a "power-pruning" algorithm, in which the subchannels were initially allocated power according to the water-filling analogy. The power was then reduced to maintain the overall error rate when the subchannel data rates were quantised. Feig concluded that large gains over single

carrier transmission could be achieved for small error rates over channels whose frequency characteristics are far from uniform. In [32]–[35], a more theoretical approach to optimising OFDM was presented.

The first commercial modem to have been designed using variable assignment multicarrier modulation was the Telebit® Trailblazer which transmitted up to 18 kbps half duplex over leased voiceband telephone channels. The voiceband is divided into 512 subchannels of which only the best 400 are used. The modulation is QAM using 4, 16 or 64 point constellations, depending on the attenuation of the subchannel [15].

1.4 MULTIUSER MULTICARRIER SYSTEMS

A multicarrier system for multiple users is configured so subsets of the available subcarriers are allotted to different users. On the uplink path (i.e. user to base-station) the time synchronisation may not be perfect, and signals from different users will not all arrive at the same instant in time. Additionally, unequal offsets in the frequencies of the users' transmitters will cause all of the subcarriers associated with a given user to shift relative to all other users' frequencies. The consequence is that adjacent-user interference is experienced in the receiver, as orthogonality properties amongst the subcarriers are lost and the receiver is not able to separate the different subcarrier signals. Non-linearities in the transmission system (e.g. due to amplifier saturation) will also cause a loss of subcarrier orthogonality.

1.5 OUTLINE

This technical note assembles the work published in [33]–[35], addressing the theoretical approach to optimising OFDM. This is enhanced by a section on multiuser multicarrier, which considers the impact of neighbouring users on optimal data and power assignment. A more practical approach to achieve nearly optimal OFDM is also presented.

In Sec. 2 the problem of optimising the data and power assignments to each of the OFDM subchannels is carefully examined. The data and power allocation is optimised to achieve the maximum possible data rate for a given transmitter power and pre-specified performance without an assumption of equal reliability on each of the subchannels. An algorithm is presented for achieving this maximum throughput.

In previous work, the reliability criterion has been the overall error probability. This allows direct comparison of OFDM transmission with single carrier transmission using equalisers designed using the zero-forcing principle. It is proved here that optimum OFDM transmission will always perform at least as well as equalised single carrier transmission using either a linear or a decision feedback equaliser. The error probability criterion is considered in Sec. 3.

A new criterion was introduced in [33] which allows comparison with single carrier systems using equalisers designed using the minimum mean-square error (MMSE) principle. With this criterion, it is seen that optimum OFDM will always achieve a data rate at least that of a single carrier using a linear MMSE equaliser. At low and intermediate SNRs, significant increases in data rate are also achieved compared to the decision feedback equalised single carrier. This new criterion is considered in Sec. 4.

In Sec. 5, an AWGN channel example is used to demonstrate that significant improvements in data rate can be realised using optimum OFDM transmission over channels with poor signal-to-noise ratios and/or large variations in channel gain across the bandwidth.

The case of a multi-user multicarrier system is considered in Sec. 6, where the effects of adjacent band interference on the allocation of power and data are evaluated.

The algorithmic solution given in Sec. 2, while yielding the optimum allocations, may be slow to converge, and is not suggested for use in practical OFDM applications. A more practical approach to optimising OFDM is presented in Sec. 7.

2 MULTICARRIER TRANSMISSION

Kalet [17, 18] stated that the symbol error rates must be uniform across the subchannels for optimum performance. In [17], he considered two subchannels and found, incorrectly, that the bandwidth efficiency was maximised when the power was uniformly distributed, regardless of the relative attenuations of the two subchannels. In [18] this was revised, but the condition of equal symbol error rates was maintained. In considering more subchannels, [18], Kalet used the constraint that all subchannels must transmit at least two bits per modulating symbol, but clearly there are circumstances in which not all subchannels are usable and no method of determining which subchannels fit this criterion was given.

Bingham [4] stated that it was intuitively reasonable that the requirement for optimum performance was the equi-distribution of bit error rates among the subchannels. He said that the ideal power distribution should be determined using the "water-pouring" method that Gallager described for achieving channel capacity [14, sec.8.3].

In this study, the assumption of uniform performance (either bit or symbol error rate) is eliminated. The performance optimisation problem will be stated in the form of a constrained minimisation. The resulting solution yields conditions for the optimum distribution of power and data which are not met by either Kalet's or Bingham's requirements. These conditions can be achieved using an iterative algorithm to assign the transmission power and data among the subchannels. The algorithm can easily be constrained to allow at least two bits per modulating symbol on each subchannel without *a priori* specification of the number of subchannels to be used.

A lower bound on maximum achievable transmission rate is found for Quadrature Amplitude Modulation (QAM) which facilitates comparison of the OFDM system with equalised single carrier QAM systems. The OFDM system is shown to outperform single carrier QAM using either a linear or a nonlinear (decision feedback) equaliser.

Prior to the initialisation of this study, all previous work in the area of multicarrier performance optimisation used the error probability criterion. However, in the development and optimisation of equalisers for single carrier transmission, the mean-square error (MSE) has proved valuable as a tractable design criterion. In this work, a new criterion based on the MSE has been introduced which allows direct comparison with single carrier transmission systems using equalisers designed using the minimum mean-square error (MMSE) principle. Multicarrier transmission is shown to achieve higher data rates than linearly equalised single carrier QAM, but the analytical results for this criterion compared to a single carrier using a DFE are inconclusive.

2.1 SYSTEM MODEL

The linearly dispersive channel under consideration is modelled by a bandpass filter with transfer function $X(f)$, where $X(f) \neq 0$ over some frequency range spanning W Hz, corrupted by additive Gaussian noise. The noise has power spectral density $N(f)$ and is modelled as the output of a linear filter $H_N(f)$ excited by white Gaussian noise with zero mean and two-sided power spectral density $\frac{N_0}{2}$ W/Hz. The first stage of the receiver consists of a matched filter $G(f) = X^*(f)$. The channel model is shown in Fig. 2.1.

The equivalent model is a filter $H(f) = X(f)G(f)$ with coloured Gaussian noise, $\eta(t)$, at the receiver. The noise variance is given by

$$\sigma_\eta^2 = \frac{N_0}{2} \int_{-\infty}^{\infty} |H_N(f)G(f)|^2 \, df. \tag{2.1}$$

The data is transmitted in blocks of R_b bits. Each block is divided into Z sub-blocks of b_i bits, $i = 1, \ldots, Z$, such that $R_b = \sum_{i=1}^{Z} b_i$, which are used to modulate Z subcarriers at frequencies f_i separated by W_Z Hz, $W_Z = \frac{1}{Z}W$. At the receiver, the subcarriers are demodulated synchronously and the signals are sampled at intervals $T_Z = \frac{1}{W_Z}$. The Z received bit sequences are then reassembled in their original order (Fig. 1.1). In practice, this operation could be carried out using a discrete Fourier transform (DFT) or block demodulator. The overall system is transmitting an R_b-bit block of data every T_Z seconds, thus the overall bit rate is $\frac{1}{Z}R_bW$ bits/s.

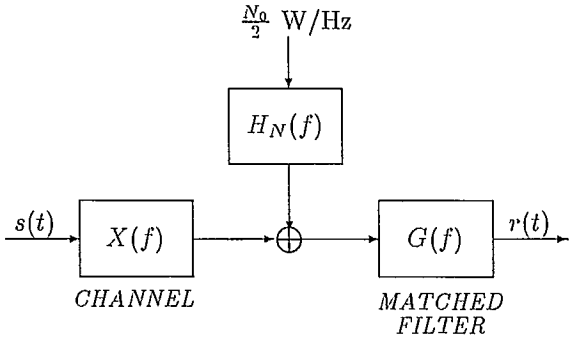

Figure 2.1: Channel model

Although it is more usual to consider attenuation-noise characteristics, in this case the gain-noise ratio is more tractable in the subsequent analysis. The channel gain-noise characteristics are assumed to be piece-wise constant, i.e.

$$\left|\frac{X(f)}{H_N(f)}\right|^2 = k_i \qquad \text{for} \qquad |f - f_i| < \frac{W_Z}{2}$$

as illustrated in Fig. 2.2. The received SNR for the b_i-bit symbol transmitted on the ith subchannel with power P_i is therefore $\gamma_{r,i} = \frac{P_i k_i}{N_0 W_Z}$.

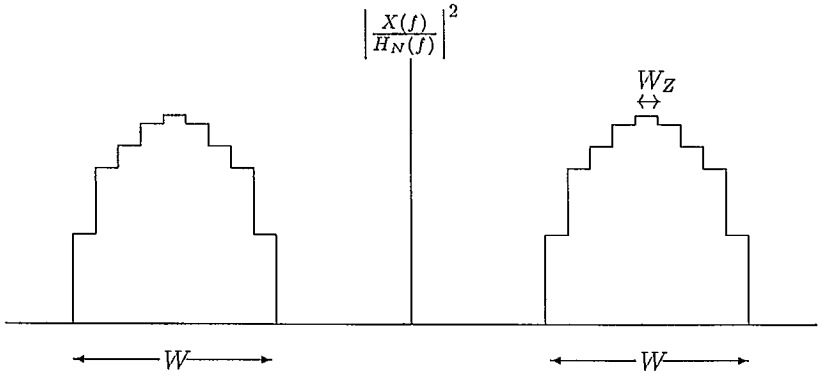

Figure 2.2: Channel response

For the purposes of this analysis, it is assumed that no guard bands are used. This assumption does not affect the results if coherent detection over the whole symbol period is considered.

2.2 PERFORMANCE CRITERIA

The criterion of performance used in practice, and in earlier work [8, 9] is the error probability criterion. This criterion provides a basis for comparing multicarrier transmission with single carrier transmission using an equaliser designed according to the zero-forcing principle to minimise intersymbol interference (ISI).

A new criterion for measuring the performance of the multicarrier system, the normalised mean-square error (NMSE), was presented in [33, 35] where it was called the mean-square signal separation (MSSS) ratio. It is based on the MSE, and can be used to compare multicarrier transmission with single carrier transmission using equalisers designed using the MMSE principle. These equalisers have better noise properties than those designed to minimise ISI and are therefore more frequently used in data communications.

2.2.1 Error probability criterion

The objective here, as in previous work, for example [4, 17, 18], is to maximise the data throughput, R_b, of the multicarrier system for a given total transmission power, $\sum_{i=1}^{Z} P_i = P_{max}$, such that the received data achieves a specified overall bit error probability, $p_e = p_{max}$.

Using Gray-coded symbols, for small error probabilities on each subchannel, the probability of more than one bit error resulting from a symbol detection error is negligible. Therefore, denoting the bit and symbol error probabilities on the ith subchannel as p_i and s_i respectively, the overall bit error probability is given by

$$p_e = \frac{\sum_{i=1}^{Z} b_i p_i}{\sum_{i=1}^{Z} b_i} = \frac{\sum_{i=1}^{Z} s_i}{R_b}. \tag{2.2}$$

In practice, not all the subchannels need be used. On those subchannels where $b_i = 0$ and $P_i = 0$, the values of p_i and s_i in (2.2) will be taken to be zero.

2.2.2 NMSE criterion

The normalised mean-square error (NMSE) criterion is the mean-square error of the received signal normalised by the signal energy. In [19], where the transmitted signals were coset coded, the requirement that the minimum squared distance between adjacent points was equal across the subchannels was specified. It will be seen that on subchannels with different gain-to-noise characteristics, neither the data nor the power will be uniformly distributed for optimum performance. As both the error and the signal energies per bit are dependent on the power and data rate, the ratio of these measures is a more useful measure of performance.

On subchannel i, adjacent points x and y in the received signal constellation for ideal (i.e. noise-free) transmission are separated by a distance $2\rho_i(x, y) = 2|x - y|$. Over the M_i constellation points, the *mean-square modulation distance* is then defined as

$$d_i^2 \triangleq E\left\{\rho_i(x, y)^2\right\}. \tag{2.3}$$

The *mean-square error* at the system output on subchannel i is found from

$$\sigma_i^2 = E\left\{\left|a_{n,i} - \tilde{a}_{n,i}\right|^2\right\} \tag{2.4}$$

where $a_{n,i}$ is the actual transmitted data symbol at time nT_Z and $\tilde{a}_{n,i}$ is the corresponding input to the threshold detector.

The *normalised mean-square error* on subchannel i for b_i bits per sub-block is defined by

$$\varepsilon_i \triangleq \frac{\sigma_i^2}{d_i^2}. \tag{2.5}$$

Over the Z subchannels, the average normalised mean-square error per bit is then

$$\epsilon = \frac{\sum_{i=1}^{Z} \frac{\sigma_i^2}{d_i^2}}{\sum_{i=1}^{Z} b_i} = \frac{\sum_{i=1}^{Z} \varepsilon_i}{R_b}. \tag{2.6}$$

The optimisation objective is to maximise the number of bits per block, R_b, for a given transmitter power, P_{max}, such that the average normalised mean-square error per bit at the receiver, ϵ, is equal to some given value ϵ_{max}. As in Sec. 2.2.1, σ_i^2 and ε_i will be given the value zero on subchannels for which $b_i = 0$.

2.3 TRANSMISSION OPTIMISATION

In this section, the conditions for optimum transmission are derived for a general criterion which has the value ϑ_i on subchannel i, and an average of θ per bit across all the subchannels. The objective is to maximise the data throughput of the system, R_b, by optimising the allocation of power and data rates among the subchannels, such that the performance criterion, θ, satisfies the constraint

$$\theta = \frac{\sum_{i=1}^{Z} \vartheta_i}{R_b} = \theta_{max} \tag{2.7}$$

where the parameter ϑ_i is assigned the value zero for any subchannel i on which $b_i = 0$. For the error probability criterion $\theta = p_e$ and $\vartheta_i = s_i$, while for the NMSE criterion $\theta = \epsilon$, $\vartheta_i = \varepsilon_i$.

The b_i's are assumed to be continuously variable for the purposes of analysis. Define $\boldsymbol{b}$ to be the N-dimensional vector of non-zero b_i's and $\boldsymbol{P}$ to be the vector of corresponding P_i's. The optimisation problem can then be stated:

$$\text{maximise} \qquad R_b = \sum_{i=1}^{Z} b_i \qquad w.r.t. \qquad \boldsymbol{b},\ \boldsymbol{P} \in \Re^N \tag{2.8}$$

$$\text{subject to} \qquad h_1 = \sum_{i=1}^{Z} P_i - P_{max} = 0 \tag{2.9}$$

$$h_2 = \theta - \theta_{max} = 0 \tag{2.10}$$

Using the Lagrange multiplier method [2, p.67], the Lagrangian function is defined as

$$L(\boldsymbol{b}, \boldsymbol{P}, \boldsymbol{\lambda}) \triangleq -R_b + \boldsymbol{\lambda}^T \boldsymbol{h} \tag{2.11}$$

where $\boldsymbol{\lambda} = [\lambda_1\ \lambda_2]^T$ is the vector of Lagrange multipliers and $\boldsymbol{h} = [h_1\ h_2]^T$ is the constraint vector.

The vectors $\boldsymbol{b}$ and $\boldsymbol{P}$ are optimum when

$$\nabla L(\boldsymbol{b}^*, \boldsymbol{P}^*, \boldsymbol{\lambda}) = -\nabla R_b + \boldsymbol{\lambda}^T \nabla \boldsymbol{h} = 0 \tag{2.12}$$

where an asterix denotes an optimum value. The solution found is a strict global minimum if the Hessian

$$\nabla^2 L(\boldsymbol{b}, \boldsymbol{P}, \boldsymbol{\lambda}) = -\nabla^2 R_b + \boldsymbol{\lambda}^T \nabla^2 \boldsymbol{h} \tag{2.13}$$

is positive semi-definite [21, chap.10], i.e. the Lagrangian function is convex.

Equation (2.12) yields

$$-\left.\frac{\partial R_b}{\partial b_i}\right|_{\{b^*,P^*\}} + \lambda_1 \left.\frac{\partial P_{max}}{\partial b_i}\right|_{\{b^*,P^*\}} + \lambda_2 \left.\frac{\partial \theta}{\partial b_i}\right|_{\{b^*,P^*\}} = 0 \tag{2.14}$$

$$-\left.\frac{\partial R_b}{\partial P_i}\right|_{\{b^*,P^*\}} + \lambda_1 \left.\frac{\partial P_{max}}{\partial P_i}\right|_{\{b^*,P^*\}} + \lambda_2 \left.\frac{\partial \theta}{\partial P_i}\right|_{\{b^*,P^*\}} = 0 \tag{2.15}$$

over all i such that $b_i \neq 0$. Since $R_b = \sum_{i=1}^{Z} b_i$ is independent of the power distribution $\boldsymbol{P}$ and $P_{max} = \sum_{i=1}^{Z} P_i$ is independent of the data allocation $\boldsymbol{b}$, (2.14) and (2.15) give, for all i such that $b_i \neq 0$,

$$-1 + \lambda_2 \left.\frac{\partial \theta}{\partial b_i}\right|_{\{b^*,P^*\}} = 0 \tag{2.16}$$

$$\lambda_1 + \lambda_2 \left.\frac{\partial \theta}{\partial P_i}\right|_{\{b^*,P^*\}} = 0 \tag{2.17}$$

Therefore the optimum solution is found by solving the gradient conditions

$$\left.\frac{\partial\theta}{\partial b_i}\right|_{\{b^*,P^*\}} = \xi_1 \tag{2.18}$$

$$\left.\frac{\partial\theta}{\partial P_i}\right|_{\{b^*,P^*\}} = \xi_2 \tag{2.19}$$

for all i such that $b_i \neq 0$, where ξ_1 and ξ_2 are constants, such that $R_b = \sum_{i=1}^{Z} b_i$, $P_{max} = \sum_{i=1}^{Z} P_i$ and $\theta = \theta_{max}$.

The conditions derived above for optimum transmission hold for systems distorted by additive noise, ISI and interchannel interference (ICI).

2.3.1 Algorithmic solution

The conditions found for optimum performance, (2.18) and (2.19), often cannot be solved explicitly but require an iterative solution. The number of subchannels on which transmission takes place in the optimum case, N, may not be known *a priori*. The optimisation of the transmission is therefore performed using a steepest descent algorithm to assign the data and power among the subchannels.

Considering (2.14) and (2.15), it is seen that the problem of maximising R_b for a given value of θ is essentially the same as minimising θ for a fixed value of R_b. This observation yields an algorithmic solution which, while it does not necessarily have the fastest possible convergence, is readily adaptable to different criteria and additional constraints, for example setting a minimum number of bits per sub-block or requiring only integer-valued data rates.

After the initialisation, during which all the transmitter power is assigned to the subchannels and the data rates are chosen such that $\theta = \theta_{max}$, the optimisation can be broken into two sub-problems, i.e. minimise θ with respect to (i) the sub-block size and (ii) the power distribution. The overall data rate is increased at each step to ensure the criterion constraint, (2.10), is met, i.e. that the solution is feasible.

These sub-problems are solved using a modified reduced gradient method, the convex simplex technique [21, sec.11.8]. In this method, the change in θ is calculated when a small value of the parameter, i.e. Δb or ΔP, is transferred from one subchannel to another. The change that results in the largest decrease in θ is implemented, and the process is repeated.

The function θ may be nonlinear so to simplify the minimisation linear approximations are made to the change in θ for unilateral increments and decrements of Δb or ΔP. Thus the following values are defined

$$\Delta\theta^-_{b,i} = \left[\vartheta_i|_{\{b_1,\ldots,b_i,\ldots,b_Z,\boldsymbol{P}\}} - \vartheta_i|_{\{b_1,\ldots,b_i-\Delta b,\ldots,b_Z,\boldsymbol{P}\}}\right] \tag{2.20}$$

$$\Delta\theta^+_{b,i} = \left[\vartheta_i|_{\{b_1,\ldots,b_i+\Delta b,\ldots,b_Z,\boldsymbol{P}\}} - \vartheta_i|_{\{b_1,\ldots,b_i,\ldots,b_Z,\boldsymbol{P}\}}\right] \tag{2.21}$$

$$\Delta\theta^-_{P,i} = \left[\vartheta_i|_{\{\boldsymbol{b},P_1,\ldots,P_i,\ldots,P_Z\}} - \vartheta_i|_{\{\boldsymbol{b},P_1,\ldots,P_i-\Delta P,\ldots,P_Z\}}\right] \tag{2.22}$$

$$\Delta\theta^+_{P,i} = \left[\vartheta_i|_{\{\boldsymbol{b},P_1,\ldots,P_i+\Delta P,\ldots,P_Z\}} - \vartheta_i|_{\{\boldsymbol{b},P_1,\ldots,P_i,\ldots,P_Z\}}\right] \tag{2.23}$$

The optimisation algorithm can then be described as follows.

Step 1 • Initialisation

The system is initialised at a feasible solution, i.e. the number of bits per sub-block and the power assigned to each subchannel are chosen such that the constraints given by (2.9) and (2.10) are met.

For example, this can be implemented by setting the value of $\vartheta_i = \theta_{max}$ across all the subchannels, and allocating power in such a way as to maximise the overall data rate.

Step 2 • Sub-problem (i): minimise θ w.r.t. $\mathbf{b}_i$'s

For each subchannel, calculate the terms $\Delta\theta^+_{b,i}$ and $\Delta\theta^-_{b,i}$ for the current value of Δb.

$\star$ Find the subchannels I and J such that

$$\Delta\theta^+_{b,I} = \overset{min}{i}\ \Delta\theta^+_{b,i} \qquad \text{and} \qquad \Delta\theta^-_{b,J} = \overset{min}{i}\ \Delta\theta^-_{b,i} \tag{2.24}$$

where $\Delta\theta^+_{b,I} > 0$, $\Delta\theta^-_{b,J} < 0$ and $I \neq J$. Then, if

$$\left|\Delta\theta^+_{b,I}\right| < \left|\Delta\theta^-_{b,J}\right| \tag{2.25}$$

transferring Δb from subchannel J to I will result in the largest overall decrease in θ. Therefore increment b_I by Δb and decrement b_J by the same amount. Recalculate $\Delta\theta^+_{b,I}$, $\Delta\theta^-_{b,I}$, $\Delta\theta^+_{b,J}$ and $\Delta\theta^-_{b,J}$.

Repeat from $\star$ until $\left|\Delta\theta^+_{b,I}\right| \geq \left|\Delta\theta^-_{b,J}\right|$, i.e. no further transfer will reduce θ.

Step 3 • Find nearest feasible solution of $\mathbf{b}_i$'s

The constraint $\theta = \theta_{max}$ no longer holds, therefore the current solution is not feasible. This is corrected by increasing the overall data rate until the constraint is satisfied.

$\star$ Find the subchannel I such that

$$\Delta\theta^+_{b,I} = \overset{min}{i}\ \Delta\theta^+_{b,i} \tag{2.26}$$

Then, if $\Delta\theta^+_{b,I} \leq \theta_{max} - \theta$, increasing the number of bits in sub-block I will result in the smallest overall increase in θ. Increment b_I by Δb, and recalculate $\Delta\theta^+_{b,I}$.

Repeat from $\star$ until $\Delta\theta^+_{b,I} > \theta_{max} - \theta$, i.e. no further increases in the data rate can be made.

Step 4 • Sub-problem (ii): minimise θ w.r.t. $\mathbf{P}_i$'s

For each subchannel, calculate the terms $\Delta\theta^+_{P,i}$ and $\Delta\theta^-_{P,i}$ for the current value of ΔP.

$\star$ Find the subchannels I and J such that

$$\Delta\theta^+_{P,I} = \overset{min}{i}\ \Delta\theta^+_{P,i} \qquad \text{and} \qquad \Delta\theta^-_{P,J} = \overset{min}{i}\ \Delta\theta^-_{P,i} \tag{2.27}$$

where $\Delta\theta^+_{P,I} < 0$, $\Delta\theta^-_{P,J} > 0$ and $I \neq J$. Then, if

$$\left|\Delta\theta^+_{P,I}\right| > \left|\Delta\theta^-_{P,J}\right| \tag{2.28}$$

transferring ΔP from subchannel J to I will result in the largest overall decrease in θ. Therefore increment P_I by ΔP and decrement P_J by the same amount. Recalculate $\Delta\theta^+_{P,I}$, $\Delta\theta^-_{P,I}$, $\Delta\theta^+_{P,J}$ and $\Delta\theta^-_{P,J}$.

Repeat from $\star$ until $\left|\Delta\theta^+_{P,I}\right| \leq \left|\Delta\theta^-_{P,J}\right|$, i.e. no further transfer will reduce θ.

Step 5 • Find nearest feasible solution of $\mathbf{b}_i$'s

Repeat step 3.

These steps are repeated until no further changes are made to the b_i's and P_i's. The usual modifications can be made to Δb and ΔP to speed up convergence while achieving a sufficiently accurate solution, for example by using large increments initially and reducing them at each iteration.

It can be seen that as Δb, $\Delta P \to 0$, the transfer of parameters among the subchannels ceases when

$$\frac{\partial\theta}{\partial b_i} = \frac{\partial\theta}{\partial b_j} \qquad \text{and} \qquad \frac{\partial\theta}{\partial P_i} = \frac{\partial\theta}{\partial P_j} \qquad \forall\ i,\ j \text{ s.t. } b_i, b_j \neq 0 \tag{2.29}$$

which are the optimum conditions derived using the Lagrange multiplier method, (2.18) and (2.19). Therefore, if the requirement that θ is convex with respect to all non-zero b_i's and P_i's is met, the solution found using this algorithm tends to the optimum solution.

Note that by including all subchannels in the sub-problems (steps 2 and 4), and subject to the obvious condition that b_i, $P_i \geq 0$, the problem of determining N, the number of subchannels used for transmission, *a priori* is avoided.

2.4 CAPACITY

From [14, sec.8.5], the capacity (in bits/s) of the additive Gaussian noise channel of Fig. 2.1, in which the power and bandwidth of the signal are constrained, is given by

$$C = \int_{f \in F_B} \frac{1}{2} \log_2 \left[\frac{|X(f)G(f)|^2 B}{|H_N(f)G(f)|^2 N_0} \right] df \tag{2.30}$$

where F_B is the set of frequencies for which $B \geq \frac{|H_N(f)|^2 N_0}{|X(f)|^2}$ and B is the solution to

$$P_{max} = \int_{f \in F_B} \left[B - \frac{|H_N(f)|^2 N_0}{|X(f)|^2} \right] df. \tag{2.31}$$

As in Sec. 2.1, $H(f) = X(f)G(f)$, and the channel and filter responses are piece-wise constant and two-sided. The gain-noise factor is

$$k_i = \left| \frac{X(f)}{H_N(f)} \right|^2 \qquad \text{for} \qquad |f - f_i| < \frac{W_Z}{2}.$$

The capacity equations can therefore be rewritten

$$C = \sum_{i \in I_B} \log_2 \left[\frac{k_i B}{N_0} \right] W_Z \tag{2.32}$$

and

$$P_{max} = \sum_{i \in I_B} \left[B - \frac{N_0}{k_i} \right] W_Z \tag{2.33}$$

where I_B is the set of i such that $B \geq \frac{N_0}{k_i}$.

The distribution of transmission power among the subchannels required to achieve capacity is found from $\sum_{i=1}^{Z} P_{C,i} = P_{max}$ where

$$P_{C,i} = \begin{cases} \left(B - \frac{N_0}{k_i} \right) W_Z & i \in I_B \\ 0 & \text{otherwise} \end{cases} \tag{2.34}$$

The capacity of each subchannel, C_i, can then be written

$$C_i = \log_2 \left[1 + \frac{P_{C,i} k_i}{N_0 W_Z} \right] W_Z = \log_2 \left[1 + \gamma_{C,i} \right] W_Z \tag{2.35}$$

where $\gamma_{C,i}$ is the received SNR on the ith subchannel, and the total channel capacity is given by $C = \sum_{i=1}^{Z} C_i$. Equation (2.35) is the Shannon equation of capacity [14, sec.8.3] which applies because the assumption of piece-wise constant channel and filter characteristics ensures the noise on each subchannel is white.

3 ERROR PROBABILITY CRITERION

Applying the error probability criterion, $\theta = p_e$, from (2.18) and (2.19), the conditions for optimum distribution of transmission power and data are

$$\left.\frac{\partial p_e}{\partial b_i}\right|_{\{b^*,P^*\}} = \xi_1 \tag{3.1}$$

$$\left.\frac{\partial p_e}{\partial P_i}\right|_{\{b^*,P^*\}} = \xi_2 \tag{3.2}$$

Using (2.2), as $\frac{\partial R_b}{\partial b_i} = 1$, these give

$$\frac{\partial p_e}{\partial b_i} = \frac{R_b \sum_{j=1}^{Z} \frac{\partial s_j}{\partial b_i} - \sum_{j=1}^{Z} s_j}{R_b^2} = \frac{1}{R_b}\left[\sum_{j=1}^{Z} \frac{\partial s_j}{\partial b_i} - p_e\right] \tag{3.3}$$

and

$$\frac{\partial p_e}{\partial P_i} = \frac{1}{R_b} \sum_{j=1}^{Z} \frac{\partial s_j}{\partial P_i} \tag{3.4}$$

Therefore the conditions become

$$\sum_{j=1}^{Z} \frac{\partial s_j}{\partial b_i} = \zeta_1 \quad \text{and} \quad \sum_{j=1}^{Z} \frac{\partial s_j}{\partial P_i} = \zeta_2 \tag{3.5}$$

where ζ_1 and ζ_2 are constants. When the system is designed for no interchannel interference,

$$\frac{\partial s_j}{\partial b_i} = \frac{\partial s_j}{\partial P_i} = 0 \quad \forall\ j \neq i \text{ s.t. } b_i, b_j \neq 0 \tag{3.6}$$

therefore (3.5) can be simplified to

$$\left.\frac{\partial s_i}{\partial b_i}\right|_{\{b_i^*,P_i^*\}} = \zeta_1 \quad \text{and} \quad \left.\frac{\partial s_i}{\partial P_i}\right|_{\{b_i^*,P_i^*\}} = \zeta_2. \tag{3.7}$$

These conditions are not met by setting either the symbol ($s_i = b_i p_i$) or the bit (p_i) error probabilities equal across the subchannels used, except in the special case when the subchannel attenuations are equal (i.e. the overall Nyquist I channel).

3.1 OPTIMUM QAM TRANSMISSION

When N of the Z subchannels are used, the transmitted signal consists of N orthogonal M_i-ary QAM signals of the form

$$x_i(t) = \sum_{n=-\infty}^{\infty} Re\{a_{n,i}\} s_i(t - nT_Z) \cos 2\pi f_i t + Im\{a_{n,i}\} s_i(t - nT_Z) \sin 2\pi f_i t \tag{3.8}$$

where the complex data points $\{a_{n,i}\}$ are taken from the $M_i = 2^{b_i}$ point signal constellation, and f_i is the ith subcarrier frequency, as in Sec. 2.1. The baseband signal $s_i(t)$ is assumed to be ISI-free at the sampling instant, and the subchannel is assumed to be flat-topped across its bandwidth W_Z.

Without loss of generality, it will be assumed that the subchannels are ordered such that $k_i \geq k_j$ for $i < j$. Thus $b_i \neq 0$, $P_i \neq 0$ for $i = 1, \ldots, N$.

For coherent detection of QAM in a practical digital communications system, the symbol error probability is given by [26, sec.4.2]

$$s_i = K_i erfc\left(\sqrt{\frac{3P_i k_i}{2N_0 W_Z (M_i - 1)}}\right) \tag{3.9}$$

where to simplify the optimisation, the dependence of $K_i = 2\left(1 - \frac{1}{\sqrt{M_i}}\right)$ on b_i will be neglected. As the signals are orthogonal and the subchannel model is flat-topped, it is assumed that the N received QAM signals are free of ISI and ICI at the sampling instants.

The results of the constrained optimisation can be applied to the problem of maximising the data throughput for this system for a given overall bit error probability, p_{max}, provided that p_e is convex with respect to $\boldsymbol{b}$ and $\boldsymbol{P}$, defined in Sec. 2.3. It is shown in Appendix A.1 that the condition for convexity is that w_i satisfies

$$w_i^2 \geq \frac{3P_i k_i}{2N_0 W_Z \left(\frac{3P_i k_i}{N_0 W_Z} - 3\right)} > \frac{1}{2}. \tag{3.10}$$

Therefore, for practical values of SNR and error probability, the assumption of convexity is valid.

The optimum conditions for this multicarrier QAM transmission with no ICI are therefore

$$\frac{\partial s_i}{\partial b_i} = K_i \frac{\ln 2}{\sqrt{\pi}} \frac{M_i}{M_i - 1} w_i e^{-w_i^2} = \zeta_1 \tag{3.11}$$

and

$$\frac{\partial s_i}{\partial P_i} = -K_i \frac{1}{\sqrt{\pi}} \frac{w_i}{P_i} e^{-w_i^2} = \zeta_2 \tag{3.12}$$

for $i = 1, \ldots, N$, where $w_i = \sqrt{\frac{3P_i k_i}{2N_0 W_Z (M_i - 1)}}$. Clearly the required parameters b_i (or M_i) and P_i are not explicitly determinable from these conditions, and hence R_b cannot be calculated directly. The algorithm of Sec. 2.3.1 can be applied to calculate the optimum distribution of data and power iteratively.

3.2 LOWER BOUND ON PERFORMANCE

As discussed in Sec. 2.3.1, if the derivative conditions are violated but the constraints are not, the solution found will be feasible but not optimal. A lower bound on the maximum transmission rate can therefore be found by making two approximations. The first is to upper-bound K_i, i.e. set $K_i = K = 2$. As s_i is monotonically increasing with b_i, any solution involving s_i will thereby underestimate the optimum solution R_b^*.

The second approximation is to assume that the symbol error probabilities are constant across the subchannels, i.e. $s_i = s$ for $i = 1, \ldots, Z$. This violates the derivative conditions, (3.11) and (3.12), for optimising R_b, hence the solution found will be a lower bound if the constraints $\sum_{i=1}^{Z} P_i = P_{max}$ and $p_e = p_{max}$ are met. This condition was stated to be optimum in [17] and [18].

The error function can be upper-bounded [1]

$$erfc(x) = \frac{2}{\sqrt{\pi}} \int_x^\infty e^{-t^2}\, dt \leq \frac{2}{\sqrt{\pi}} \frac{e^{-x^2}}{x + \sqrt{x^2 + \frac{4}{\pi}}} \tag{3.13}$$

therefore

$$s = s_i = K erfc(w_i) < \frac{K e^{-w_i^2}}{\sqrt{\pi} w_i}. \tag{3.14}$$

The lower bound is then found when w_i is constant across the subchannels used, i.e. $\frac{P_i k_i}{M_i - 1} = const.$ The derivative conditions for optimum transmission are then approximated by

$$\zeta_1 \approx \ln 2 \frac{M_i}{M_i - 1} w_i^2 \frac{K e^{-w_i^2}}{\sqrt{\pi} w_i} > \ln 2 \frac{M_i}{M_i - 1} w_i^2 s = \tilde{\zeta}_1 \tag{3.15}$$

$$\zeta_2 \approx -\frac{w_i^2}{P_i}\frac{Ke^{-w_i^2}}{\sqrt{\pi}w_i} < -\frac{w_i^2}{P_i}s = \tilde{\zeta}_2 \tag{3.16}$$

As $w_i^2 = \frac{3P_ik_i}{2N_0W_Z(M_i-1)}$, (3.16) yields $\frac{k_i}{M_i-1} = const$ and consequently $P_i = const$ from (3.14). Therefore for the lower bound the power distribution is uniform across the subchannels, i.e. $P_i = \frac{1}{Z}P_{max}$.

From (3.9),

$$\frac{M_i-1}{k_i} = \frac{3P_i}{2N_0W_Z}\left[erfc^{-1}\left(\frac{s_i}{K_i}\right)\right]^{-2} \tag{3.17}$$

hence substituting in the approximations and taking the geometric mean

$$\left[\prod_{i=1}^{Z}\frac{M_i-1}{k_i}\right]^{\frac{1}{Z}} = \frac{3P_{max}}{2N_0W}\left[erfc^{-1}\left(\frac{s}{K}\right)\right]^{-2}. \tag{3.18}$$

Using the inequality

$$\prod_{i=1}^{Z}(M_i-1)^{\frac{1}{Z}} \le \prod_{i=1}^{Z}M_i^{\frac{1}{Z}} - 1 = 2^{\frac{R_b}{Z}} - 1 \tag{3.19}$$

a lower bound $\bar{b}_Z = \frac{1}{Z}R_b$ on the optimum average number of bits per sub-block can be found by solving the equality in

$$2^{\bar{b}_Z} \ge 1 + \left(\prod_{i=1}^{Z}k_i\right)^{\frac{1}{Z}}\frac{3P_{max}}{2N_0W}\left[erfc^{-1}\left(\frac{\bar{b}_Z p_{max}}{K}\right)\right]^{-2}. \tag{3.20}$$

For a Nyquist I channel, i.e. $k_i = const$, the approximations used in this derivation become exact, and the inequalities used in the development of the bound become equalities. Therefore, solving (3.20) for the Nyquist I case, and using $K = 2(1-\frac{1}{\sqrt{M}})$, yields the exact solution.

3.3 EQUALISED SINGLE CARRIER TRANSMISSION

The lowpass equivalent of the channel model described in Sec. 2.1, $X_{lp}(f)$, is bandlimited to $|f| < \frac{1}{2T}$ where $T = \frac{1}{W}$ is the sampling interval. The corresponding lowpass matched filter is $G_{lp}(f) = X_{lp}^*(f)$. The linear receiver that eliminates ISI completely is the zero-forcing equaliser. This is known to perform badly on channels with poor spectral characteristics due to its noise-enhancing properties but is of general theoretical interest. The nonlinear equaliser considered is the decision feedback equaliser (DFE). The data rates of both the linear and nonlinear equalisers designed using the zero-forcing principle reduce to a form that can be readily compared to the lower bound on achievable multicarrier data rate found in Sec. 3.2.

3.3.1 Linear equaliser

The transfer function of the zero-forcing equaliser, $C(f)$, is defined by [26, sec.6.4]

$$H_{lp}(f)C(f) = 1 \qquad |f| < \frac{1}{2T} \tag{3.21}$$

where $H_{lp}(f) = X_{lp}(f)G_{lp}(f) = |X_{lp}(f)|^2$. The noise at the output of the equaliser has variance

$$\sigma_n^2 = N_0\int_{-\frac{1}{2T}}^{\frac{1}{2T}}|H_N(f)G_{lp}(f)C(f)|^2\,df = N_0\int_{-\frac{1}{2T}}^{\frac{1}{2T}}\left|\frac{H_N(f)}{X_{lp}(f)}\right|^2\,df \tag{3.22}$$

and the received signal power is P_{max}.

Since $X_{lp}(f)$ and $H_N(f)$ are piece-wise constant and $k_i = \left|\frac{X_{lp}(f)}{H_N(f)}\right|^2$ for $|f-f_i| < \frac{W_Z}{2}$, define the equivalent gain-noise factor

$$k_{zf} = \frac{W}{\int_{-\frac{1}{2T}}^{\frac{1}{2T}} |\frac{H_N(f)}{X_{lp}(f)}|^2 \, df} = \frac{W}{\sum_{i=1}^{Z} \frac{1}{k_i} W_Z} = \frac{1}{\frac{1}{Z}\sum_{i=1}^{Z} \frac{1}{k_i}}. \tag{3.23}$$

The same assumptions are made as before, namely that the symbols are Gray-coded and the SNR is sufficiently large that a symbol error results in a single bit error. Then the overall bit error probability for QAM single-carrier transmission is

$$p_e = \frac{K}{b_{zf}} erfc\left(\sqrt{\frac{3P_{max}k_{zf}}{2N_0W(2^{b_{zf}}-1)}}\right) \tag{3.24}$$

where b_{zf} is the number of bits per modulating symbol.

When the channel contains deep notches, i.e. one or more of the k_i is very small, the equivalent gain-noise factor k_{zf} approaches zero; this illustrates the noise-enhancing effects of the zero-forcing equaliser.

The data throughput of the zero-forcing equalised single carrier transmission is $b_{zf}W$ where b_{zf} solves (3.24). Therefore, from the multicarrier bit rate found in Sec. 2.1, if

$$\frac{1}{Z}R_b \geq b_{zf} \tag{3.25}$$

multicarrier transmission outperforms this single carrier transmission.

From (3.20) and (3.24), the condition for the multicarrier system to outperform the equalised single carrier system becomes

$$\left(\prod_{i=1}^{Z} k_i\right)^{\frac{1}{Z}} \frac{3P_{max}}{2N_0W}\left[erfc^{-1}\left(\frac{\bar{b}_Z p_{max}}{K}\right)\right]^{-2} \geq k_{zf}\frac{3P_{max}}{2N_0W}\left[erfc^{-1}\left(\frac{b_{zf}p_{max}}{K}\right)\right]^{-2}. \tag{3.26}$$

The error function, $erfc(x)$, decreases monotonically with x. Therefore, if $\bar{b}_Z > b_{zf}$,

$$\left[erfc^{-1}\left(\frac{\bar{b}_Z p_{max}}{K}\right)\right]^{-2} > \left[erfc^{-1}\left(\frac{b_{zf}p_{max}}{K}\right)\right]^{-2}. \tag{3.27}$$

A sufficient condition for multicarrier QAM transmission to give a better overall data rate than zero-forcing equalised single carrier QAM transmission is therefore, using (3.23)

$$\left(\prod_{i=1}^{Z} k_i\right)^{\frac{1}{Z}} \geq \frac{1}{\frac{1}{Z}\sum_{i=1}^{Z}\frac{1}{k_i}}. \tag{3.28}$$

From the inequality of means [1, sec.3],

$$\frac{1}{n}\sum_{i=1}^{n} a_i \geq \left(\prod_{i=1}^{n} a_i\right)^{\frac{1}{n}} \geq \frac{1}{\frac{1}{n}\sum_{i=1}^{n}\frac{1}{a_i}} \tag{3.29}$$

condition (3.28) holds always. The equality holds only in the special case when the k_i are constant for all i, i.e. the channel satisfies the Nyquist I criterion.

Therefore, using the error probability criterion, multicarrier transmission always outperforms single carrier transmission using a zero-forcing linear equaliser.

3.3.2 Decision feedback equaliser

The decision feedback equaliser (DFE) consists of a forward filter, $F(f)$, placed after the matched filter, $G_{lp}(f)$, and a feedback filter, $B(f)$, operating on the data sequence at the output of the threshold detector. The ideal choice of $F(f)$ to minimise the intersymbol interference has been shown [25] to be the anti-causal factor of the zero-forcing equaliser, $C(f)$, of (3.21). This whitens the noise and removes the interference due to future transmitted symbols. The coefficients of the feedback filter $B(f)$ are chosen to cancel the residual causal intersymbol interference.

The DFE suffers from error propagation, i.e. incorrect decisions result in increased ISI at the input to the threshold detector. An upper bound on the maximum achievable data rate can therefore be achieved by assuming that the feedback sequence is error-free. In this case, the error sequence at the input to the threshold detector consists only of white Gaussian noise with variance [27]

$$\sigma_n^2 = \exp\left\{-T\int_{-\frac{1}{2T}}^{\frac{1}{2T}} \ln\left(\frac{X_{lp}(f)G_{lp}(f)}{|H_N(f)|^2 N_0}\right)\, df\right\}. \tag{3.30}$$

Since the channel and filter characteristics are assumed to be piece-wise constant as before, the noise variance becomes

$$\sigma_n^2 = \exp\left\{-T\sum_{i=1}^{Z} \ln\left(\frac{k_i}{N_0}\right) W_Z\right\} \tag{3.31}$$

$$= \prod_{i=1}^{Z} \exp\left\{-\frac{1}{Z}\ln\left(\frac{k_i}{N_0}\right)\right\} = N_0 \prod_{i=1}^{Z}\left(\frac{1}{k_i}\right)^{\frac{1}{Z}}. \tag{3.32}$$

Therefore, using the same assumption as in the linear case, i.e. that a symbol error results in a single bit error, the overall bit error probability for QAM transmission using the DFE is given by (3.9) with gain-noise factor given by

$$k_{dfe} = \left(\prod_{i=1}^{Z} k_i\right)^{\frac{1}{Z}} \tag{3.33}$$

i.e.

$$p_e = \frac{K}{b_{dfe}} erfc\left(\sqrt{\frac{3P_{max}k_{dfe}}{2N_0W(2^{b_{dfe}}-1)}}\right) \tag{3.34}$$

where b_{dfe} is the number of bits per modulating symbol.

The maximum overall bit rate for a single carrier system using a zero-forcing DFE is therefore $b_{dfe}W$ bits/s where b_{dfe} is found from

$$2^{b_{dfe}} = 1 + \frac{3P_{max}k_{dfe}}{2N_0W}\left[erfc^{-1}\left(\frac{b_{dfe}p_{max}}{K}\right)\right]^{-2}. \tag{3.35}$$

Comparing (3.20) with (3.35), it is seen that upper bound on the performance of the single carrier system using the DFE is equal to the lower bound on the multicarrier system performance. Therefore, the multicarrier system will always outperform the single carrier system using the zero-forcing DFE.

At low channel SNRs, the performance of the DFE is known to degrade as error propagation worsens. At these SNRs also, the lower bound on multicarrier performance is loose, as ideal transmission will use only the subchannels with the best characteristics. The improvement in performance achieved using the multicarrier system is therefore more significant at lower channel SNRs.

3.4 TRANSMISSION OVER A NYQUIST I CHANNEL

For a channel meeting the Nyquist I criterion for zero intersymbol interference, and for no interchannel interference, the attenuation of the subchannels is uniform across the channel bandwidth, i.e. $k_i = k$, $i = 1, \ldots, Z$. From the conditions found for optimal QAM multicarrier transmission, (3.11) and (3.12), the overall transmission rate for this channel is achieved when the transmitter power P_{max} and the data block of R_b bits are both uniformly distributed among the Z subchannels.

Each subchannel is transmitting a sub-block of b_Z bits at power $\frac{P_{max}}{Z}$ and the received symbol error probability on each subchannel is

$$s = K erfc\left(\sqrt{\frac{3P_{max}k}{2N_0W(2^{bz}-1)}}\right). \tag{3.36}$$

The overall data rate is then $Zb_ZW_Z = b_ZW$ bits/s.

For single carrier transmission over the same channel, the low-pass signal is sampled at intervals $T = \frac{1}{W}$. The symbol error probability at the receiver is

$$s_{eq} = K erfc\left(\sqrt{\frac{3P_{max}k}{2N_0W(2^{b_{eq}}-1)}}\right) \tag{3.37}$$

where there are b_{eq} bits per modulating symbol. Thus the overall data rate is $\frac{1}{T}b_{eq} = b_{eq}W$ bits/s.

Since $p_e = \frac{s}{b_Z} = \frac{s_{eq}}{b_{eq}}$, the number of bits per sub-block, b_Z, equals the number of bits per modulating symbol b_{eq}. Therefore multicarrier transmission over a Nyquist I channel achieves the same maximum data rate as single carrier transmission.

4 NMSE CRITERION

In this section, the analysis for the normalised mean-square error criterion will follow closely that of Sec. 3. Applying the NMSE criterion, $\theta = \epsilon$, from (2.18) and (2.19), the optimum conditions for transmission are

$$\left.\frac{\partial \epsilon}{\partial b_i}\right|_{\{b^*,P^*\}} = \xi_1 \quad \text{and} \quad \left.\frac{\partial \epsilon}{\partial P_i}\right|_{\{b^*,P^*\}} = \xi_2 \tag{4.1}$$

Once again, if there is no ICI, this reduces to

$$\left.\frac{\partial \varepsilon_i}{\partial b_i}\right|_{\{b_i^*,P_i^*\}} = \zeta_1 \quad \text{and} \quad \left.\frac{\partial \varepsilon_i}{\partial P_i}\right|_{\{b_i^*,P_i^*\}} = \zeta_2 \tag{4.2}$$

for all i such that $b_i \neq 0$, where ζ_1 and ζ_2 are constants.

These conditions can be achieved using the iterative process presented for a general criterion.

4.1 OPTIMUM QAM TRANSMISSION

The transmitted signal is the same as that in Sec. 3.1, given by (3.8). Once again, the k_i will be assumed, without loss of generality, to be arranged in decreasing order.

The received signals are passed through a matched filter, $G(f)$, and a linear receiving filter before being sampled. The receiving filter gain on the ith subchannel is l_i, chosen to minimise the mean-square error. The assumption is made that each subchannel is flat-topped, i.e. there is no ISI, thus the sampled received signal at time nT_Z is

$$\tilde{a}_{n,i} = |X(f_i)|^2 l_i a_{n,i} + |X(f_i)|\, l_i \eta_{n,i} \tag{4.3}$$

where f_i is the subcarrier frequency, $a_{n,i}$ is the complex data symbol and $\eta_{n,i}$ is the complex noise sample at time nT_Z, where the real and imaginary parts have two-sided power spectral densities $\frac{N_0}{4}$.

The receiver gain is found by minimising the mean-square error, σ_i^2, with respect to l_i. From (2.4)

$$\begin{aligned} \sigma_i^2 &= E\left\{|a_{n,i} - \tilde{a}_{n,i}|^2\right\} \\ &= (1 - |X(f_i)|^2 l_i)^2 E\left\{|a_{n,i}|^2\right\} + |X(f_i)| l_i^2 E\left\{|\eta_{n,i}|^2\right\} \end{aligned} \tag{4.4}$$

as $E\left\{a_{n,i}\eta_{n,i}^*\right\} = 0$. Using $E\left\{|a_{n,i}|^2\right\} = \frac{P_i}{W_Z}$ and $E\left\{|\eta_{n,i}|^2\right\} = |H_N(f_i)|^2 N_0$, the optimum receiver gain is

$$l_i = \frac{\frac{P_i}{|H_N(f_i)|^2 N_0 W_Z}}{1 + \frac{P_i |X(f_i)|^2}{|H_N(f_i)|^2 N_0 W_Z}} \tag{4.5}$$

and hence the mean-square error is given by

$$\sigma_i^2 = \frac{\frac{P_i}{W_Z}}{1 + \frac{P_i |X(f_i)|^2}{|H_N(f_i)|^2 N_0 W_Z}}. \tag{4.6}$$

Adjacent points in the ideal received signal constellation are uniformly separated by $2d_i$ where d_i^2, the mean-square modulation distance, can be found from the average received signal energy

$$\frac{2(M_i - 1)d_i^2}{3} = \frac{P_i}{W_Z}(|X(f_i)|^2 l_i)^2. \tag{4.7}$$

Thus

$$d_i^2 = \frac{3P_i}{2W_Z(M_i - 1)} \left[\frac{\frac{P_i |X(f_i)|^2}{|H_N(f_i)|^2 N_0 W_Z}}{1 + \frac{P_i |X(f_i)|^2}{|H_N(f_i)|^2 N_0 W_Z}}\right]^2. \tag{4.8}$$

For the $Z-N$ subchannels, $j=N+1,\ldots,Z$, with no transmission, the value of $\varepsilon_j=\frac{\sigma_j^2}{d_j^2}$ is taken to be zero. Substituting in the gain-noise factors, k_i, the average ratio of mean-square error to mean-square modulation distance, the normalised mean-square error, across the Z subchannels is then

$$\epsilon=\frac{\sum_{i=1}^{Z}\frac{\sigma_i^2}{d_i^2}}{R_b}=\frac{1}{R_b}\sum_{i=1}^{Z}\frac{2(M_i-1)}{3}\frac{1+\frac{P_ik_i}{N_0W_Z}}{\left(\frac{P_ik_i}{N_0W_Z}\right)^2}. \tag{4.9}$$

It is shown in Appendix A.2 that the requirement for convexity in the Lagrangian function is satisfied at least for all $M_i\geq 3$, i.e. for all $b_i\geq 1.6$.

Therefore the conditions for ϵ to have a local minimum with respect to $\boldsymbol{b}$ and $\boldsymbol{P}$ are met, and the optimum values, $\boldsymbol{b}^*$ and $\boldsymbol{P}^*$, are found by solving

$$\frac{\partial\varepsilon_i}{\partial b_i}=\frac{2N_0W_Z}{3P_ik_i}\left[1+\frac{N_0W_Z}{P_ik_i}\right]\frac{R_bM_i\ln 2-M_i+1}{R_b^2}=\zeta_1 \tag{4.10}$$

and

$$\frac{\partial\varepsilon_i}{\partial P_i}=-\frac{2(M_i-1)}{3R_bP_i}\frac{N_0W_Z}{P_ik_i}\left[1+2\frac{N_0W_Z}{P_ik_i}\right]=\zeta_2. \tag{4.11}$$

These equations are not explicitly solvable, however the algorithm presented in Sec. 2.3.1 for the generalised criterion can be readily applied to calculate the optimum distributions of data and power iteratively.

4.2 LOWER BOUND ON PERFORMANCE

As in Sec. 3.2, the derivation of a lower bound on maximum achievable transmission rate is based on the approximations that each subchannel used transmits using the same transmission power and achieves the same normalised mean-square error at the receiver. Because of the convexity of the Lagrangian function, this yields a feasible but suboptimal solution, i.e. a lower bound.

The subchannels are assumed, without loss of generality, to be arranged such that the gain-noise factors, k_i, are in decreasing order. Set

$$\varepsilon_i=\frac{\sigma_i^2}{d_i^2}=\frac{2(M_i-1)}{3}\frac{N_0W_Z}{Pk_i}\left[1+\frac{N_0W_Z}{Pk_i}\right]=\varepsilon\qquad i=1,\ldots,Z \tag{4.12}$$

where $\varepsilon=\bar{b}_Z\epsilon_{max}$, $P=\frac{1}{Z}P_{max}$ and $\bar{b}_Z$ is the average number of bits per sub-block over the Z subchannels. Therefore, from (4.12), the approximate number of points in the ith signal constellation is given by

$$M_i=1+\frac{3}{2}\bar{b}_Z\epsilon_{max}\frac{Pk_i}{N_0W_Z}\frac{1}{1+\frac{N_0W_Z}{Pk_i}}=1+\frac{3}{2}\bar{b}_Z\epsilon_{max}\frac{\left(\frac{Pk_i}{N_0W_Z}\right)^2}{1+\frac{Pk_i}{N_0W_Z}}. \tag{4.13}$$

Using the inequality of means, (3.29), and the inequality of (3.19)

$$\frac{2^{\bar{b}_Z}-1}{\bar{b}_Z}\geq\frac{3}{2}\epsilon_{max}\left(\prod_{i=1}^{Z}\frac{\left(\frac{Pk_i}{N_0W_Z}\right)^2}{1+\frac{Pk_i}{N_0W_Z}}\right)^{\frac{1}{Z}}. \tag{4.14}$$

A lower bound on the optimum average number of bits per sub-block is found by solving the equality for $\bar{b}_Z$ in (4.14). The number of bits per block, R_b is then given by $Z\bar{b}_Z$. The overall transmission rate is $\bar{b}_ZW$ bits/s.

4.3 EQUALISED SINGLE CARRIER TRANSMISSION

The low pass equivalent channel model, as in Sec. 3.3, is $X_{lp}(f)$ and the corresponding matched filter is $G_{lp}(f)$. The linear and nonlinear (decision feedback) equalisers designed using the minimum mean-square error principle are widely used in data communications. In this section, upper bounds are found on the maximum achievable data rates for single carrier transmission using each of these equalisation techniques.

4.3.1 Linear equaliser

The received low pass single carrier QAM signal is sampled every T seconds before being passed through a MMSE linear equaliser. The equaliser has a transfer function [27]

$$C(f) = \frac{\mathcal{C}}{\mathcal{C}X_{lp}(f)G_{lp}(f) + N_0|H_N(f)|^2} \tag{4.15}$$

where $\mathcal{C} = E\left\{|a_n|^2\right\} = \frac{P_{max}}{W}$ is the energy of the transmitted signal.

The mean-square error at the sampler output is therefore

$$\sigma^2_{mse} = \mathcal{C}T \int_{-\frac{1}{2T}}^{\frac{1}{2T}} \frac{N_0|H_N(f)|^2}{\mathcal{C}\left|X_{lp}(f)\right|^2 + N_0|H_N(f)|^2}\, df \tag{4.16}$$

for the strictly band-limited channel.

Since $\left|\frac{X_{lp}(f)}{H_N(f)}\right|^2 = k_i$ for $|f - f_i| < \frac{1}{2}W_Z$ where $W_Z = \frac{1}{Z}W$,

$$\sigma^2_{mse} = \frac{P_{max}}{W}T\sum_{i=1}^{Z}\frac{W_Z}{1+\frac{P_{max}k_i}{N_0W}} = \frac{P_{max}}{W}\frac{1}{Z}\sum_{i=1}^{Z}\frac{1}{1+\frac{P_{max}k_i}{N_0W}}. \tag{4.17}$$

The mean-square modulation distance, d^2_{mse}, at the receiver is found from

$$\frac{2(M_{mse}-1)}{3}d^2_{mse} = \frac{P_{max}}{W}T\int_{-\frac{1}{2T}}^{\frac{1}{2T}} |X_{lp}(f)G_{lp}(f)C(f)|^2\, df \tag{4.18}$$

where $M_{mse} = 2^{b_{mse}}$ is the number of points in the signal constellation. Therefore

$$d^2_{mse} = \frac{3}{2\left(M_{mse}-1\right)}\frac{P_{max}}{W}\frac{1}{Z}\sum_{i=1}^{Z}\left(\frac{\frac{P_{max}k_i}{N_0W}}{1+\frac{P_{max}k_i}{N_0W}}\right)^2. \tag{4.19}$$

Thus the normalised mean-square error per bit is

$$\epsilon_{max} = \frac{\sigma^2_{mse}}{b_{mse}d^2_{mse}} = \frac{1}{b_{mse}}\frac{2\left(M_{mse}-1\right)}{3}\frac{\sum_{i=1}^{Z}\frac{1}{1+\frac{P_{max}k_i}{N_0W}}}{\sum_{i=1}^{Z}\left(\frac{\frac{P_{max}k_i}{N_0W}}{1+\frac{P_{max}k_i}{N_0W}}\right)^2} \tag{4.20}$$

and the maximum achievable data rate is found from

$$\frac{2^{b_{mse}}-1}{b_{mse}} = \frac{3\epsilon_{max}}{2}\frac{\sum_{i=1}^{Z}\left(\frac{\frac{P_{max}k_i}{N_0W}}{1+\frac{P_{max}k_i}{N_0W}}\right)^2}{\sum_{i=1}^{Z}\frac{1}{1+\frac{P_{max}k_i}{N_0W}}}. \tag{4.21}$$

This equalised single carrier transmission is equivalent to multicarrier transmission using a uniform allocation of data and power across all Z subchannels. This will yield a feasible but suboptimal overall data rate. Therefore, the multicarrier system will outperform the single carrier system using a linear MMSE equaliser.

4.3.2 Decision feedback equaliser

The decision feedback equaliser again consists of a feedforward filter, $F(f)$, at the output of the matched filter, and a feedback filter, $B(f)$, operating on the data sequence at the output of the threshold detector. Optimising $F(f)$ to minimise the mean-square error at the input to the threshold detector yields the anti-causal factor of the linear MMSE equaliser, given by (4.15) [31]. The coefficients of $B(f)$ are chosen to cancel the intersymbol interference due to the previously detected data symbols.

The DFE is prone to error propagation, i.e. incorrect detected symbols increase the mean-square error at the threshold detector input. To find an upper bound on the maximum throughput of the DFE, the feedback sequence is assumed to be error-free, as in Sec. 3.3.2.

A lower bound on the overall mean-square error of this DFE is given by [31]

$$\sigma_{dfe}^2 = \mathcal{C} \exp\left\{-T \int_{-\frac{1}{2T}}^{\frac{1}{2T}} \ln\left(\mathcal{C}\frac{X_{lp}(f)G_{lp}(f)}{N_0|H_N(f)|^2} + 1\right)\, df\right\}. \tag{4.22}$$

Using the gain-noise factors as before,

$$\sigma_{dfe}^2 = \frac{P_{max}}{W} \exp\left\{-T\sum_{i=1}^{Z} \ln\left(\frac{P_{max}k_i}{N_0 W} + 1\right) W_Z\right\} \tag{4.23}$$

$$= \frac{P_{max}}{W} \prod_{i=1}^{Z} \exp\left\{-\frac{1}{Z}\ln\left(\frac{P_{max}k_i}{N_0 W} + 1\right)\right\}. \tag{4.24}$$

Therefore the mean-square error at the input to the threshold detector can be written

$$\sigma_{dfe}^2 = \frac{P_{max}}{W} \prod_{i=1}^{Z} \left(\frac{1}{1+\frac{P_{max}k_i}{N_0 W}}\right)^{\frac{1}{Z}}. \tag{4.25}$$

The mean-square modulation distance is the same as for the MMSE linear equaliser, i.e.

$$d_{dfe}^2 = \frac{3}{2\left(2^{b_{dfe}}-1\right)} \frac{P_{max}}{W} \frac{1}{Z} \sum_{i=1}^{Z} \left(\frac{\frac{P_{max}k_i}{N_0 W}}{1+\frac{P_{max}k_i}{N_0 W}}\right)^2. \tag{4.26}$$

The maximum data transmission rate is therefore found by solving for b_{dfe} in

$$\frac{2^{b_{dfe}}-1}{b_{dfe}} = \frac{3\epsilon_{max}}{2} \frac{\frac{1}{Z}\sum_{i=1}^{Z}\left(\frac{\frac{P_{max}k_i}{N_0 W}}{1+\frac{P_{max}k_i}{N_0 W}}\right)^2}{\prod_{i=1}^{Z}\left(\frac{1}{1+\frac{P_{max}k_i}{N_0 W}}\right)^{\frac{1}{Z}}}. \tag{4.27}$$

Since $\frac{2^b-1}{b}$ is monotonically increasing with b, (4.14) and (4.27) can be compared directly. Using the inequality of means, (3.29),

$$\frac{1}{Z}\sum_{i=1}^{Z}\left(\frac{1}{1+\frac{P_{max}k_i}{N_0 W}}\right)^2 \geq \left(\prod_{i=1}^{Z}\frac{1}{1+\frac{P_{max}k_i}{N_0 W}}\right)^{\frac{2}{Z}} \tag{4.28}$$

therefore $b_{dfe} \geq \bar{b}_Z$, i.e. the upper bound on the data throughput for the single carrier using a DFE is greater than the lower bound on the data rate for the multicarrier system. This is inconclusive.

At low SNR, the assumption of an error-free feedback sequence in the single carrier case becomes unrealistic, i.e. the bound is loose. Also at these SNRs, not all of the subchannels will be used in the multicarrier

transmission, thus this bound is also loose. Therefore it is expected that at low SNRs, the optimised multicarrier will outperform the nonlinearly equalised single carrier. At sufficiently high SNRs, it is expected that the multicarrier system will use all the subchannels and that error propagation will have little effect on the DFE. Also at high SNRs the difference between the arithmetic and geometric means in inequality (4.28) is small, therefore the DFE may have a marginal improvement in performance compared to the optimised multicarrier, but this is somewhat speculative.

4.4 TRANSMISSION OVER A NYQUIST I CHANNEL

For multicarrier transmission over a Nyquist I channel, i.e. over Z subchannels with identical gain-noise factors k without interchannel interference, it is clear from (4.2) that the overall data rate is maximised when the transmission power P_{max} is uniformly distributed among the subchannels, and that each sub-block contains the same number of bits b_Z. In this case, the equality in (4.14) holds and the overall data rate $R_b W_Z = b_Z W$ bits/s is found by solving for b_Z in

$$\frac{2^{b_Z}-1}{b_Z} = \frac{3}{2}\epsilon_{max}\frac{\left(\frac{P_{max}k}{N_0W}\right)^2}{1+\frac{P_{max}k}{N_0W}}. \tag{4.29}$$

For single carrier transmission, the overall data rate is $b_{eq}W$ bits/s where b_{eq} is found from (4.21) or (4.27) with $k_i = k$ for $i = 1, \ldots, Z$, i.e.

$$\frac{2^{b_{eq}}-1}{b_{eq}} = \frac{3\epsilon_{max}}{2}\frac{\left(\frac{\frac{P_{max}k}{N_0W}}{1+\frac{P_{max}k}{N_0W}}\right)^2}{\frac{1}{1+\frac{P_{max}k}{N_0W}}} = \frac{3}{2}\epsilon_{max}\frac{\left(\frac{P_{max}k}{N_0W}\right)^2}{1+\frac{P_{max}k}{N_0W}}. \tag{4.30}$$

Therefore the multicarrier and single carrier transmission systems perform equally over the Nyquist I channel.

5 AWGN CHANNEL EXAMPLE

In this section, the optimisation procedure will be applied to a linearly dispersive channel with severe frequency dependent characteristics and AWGN.

The channel has transfer function $X(f)$, where $X(f)$ is bandlimited to W Hz. For simplicity, the bandwidth is normalised such that $W = 1$, thus the sampling interval $T = \frac{1}{W} = 1$. The bandwidth is divided into $Z = 256$ subchannels, and as in Sec. 2.1, the characteristics are assumed to be piece-wise constant over each subchannel bandwidth W_Z.

The noise is white, thus $H_N(f) = 1$ over the channel bandwidth. Therefore, over each subchannel i, centred at frequency f_i, the channel gain is

$$k_i = |X(f)|^2 \qquad \text{for} \qquad |f - f_i| < \frac{W_Z}{2}. \tag{5.1}$$

The gain characteristics, $|X(f)|^2$, of the model used in this example are shown in Fig. 5.1. The attenuation at the channel extremities is greater than 15 dB, and there is a mid-band notch of approximately 10 dB.

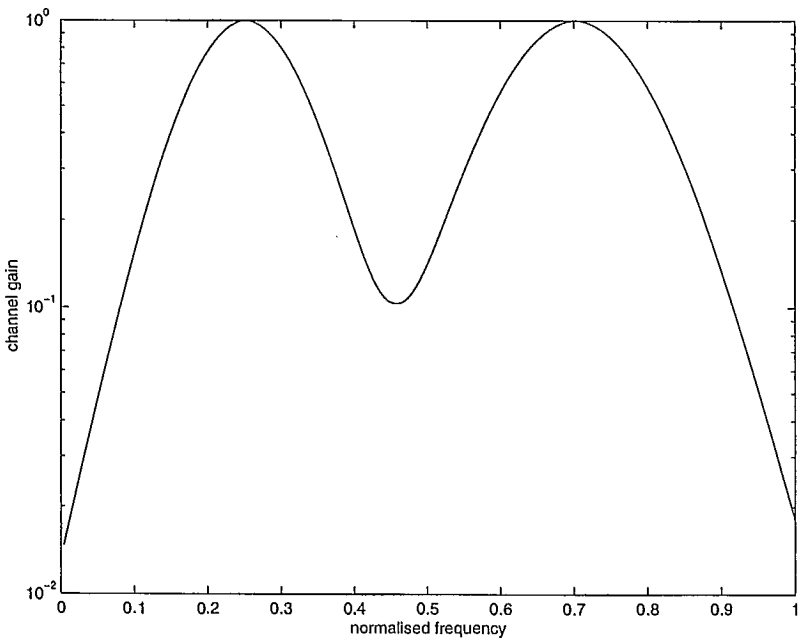

Figure 5.1: Gain of AWGN channel example, $|X(f)|^2$ over normalised bandwidth $Z = 256$ subchannels.

On subchannel i, the data is transmitted in b_i-bit blocks with an average transmission power P_i. The modulation used is QAM and the subcarrier frequency is f_i. The transmitted signal is then given by equation (3.8) where the average total transmitter power is normalised to Z W. Additive white Gaussian noise of two-sided power spectral density $\frac{N_0}{2}$ corrupts the received signal, which is passed through a matched filter, $G(f) = X^*(f)$.

At the output of the matched filter, the received signal-to-noise ratio on the ith subchannel is

$$\gamma_{r,i} = \frac{P_i k_i}{N_0 W_Z}. \tag{5.2}$$

5.1 ERROR PROBABILITY CRITERION

In Sec. 2.2.1, the overall bit error probability was given by

$$p_e = \frac{\sum_{i=1}^{Z} p_i b_i}{\sum_{i=1}^{Z} b_i} = \frac{\sum_{i=1}^{Z} s_i}{R_b} \tag{5.3}$$

where p_i and s_i are, respectively, the bit and symbol error probabilities achieved on subchannel i, and

$$s_i = K_i erfc\left(\sqrt{\frac{3P_i k_i}{2N_0 W_Z (M_i - 1)}}\right). \tag{5.4}$$

The optimum conditions for this multicarrier transmission were found in Sec. 3.1 to be

$$\frac{\partial s_i}{\partial b_i} = K_i \frac{\ln 2}{\sqrt{\pi}} \frac{M_i}{M_i - 1} w_i e^{-w_i^2} = \zeta_1 \tag{5.5}$$

and

$$\frac{\partial s_i}{\partial P_i} = -K_i \frac{1}{\sqrt{\pi}} \frac{w_i}{P_i} e^{-w_i^2} = \zeta_2 \tag{5.6}$$

where $w_i = \sqrt{\frac{3P_i k_i}{2N_0 W_Z (M_i - 1)}}$. These equations are not solvable explicitly for b_i or P_i, therefore the algorithm presented in Sec. 2.3.1 was used to determine the optimum distribution of data and power.

The results of the iterative optimisation for transmitter signal power to noise ratios of 5 to 30 dB are shown in Fig. 5.2 where the overall error probability is $p_{max} = 10^{-5}$. The plot shows the data throughput in bits/s for optimum OFDM and also for quantised OFDM, where b_i must be zero or an integer greater than two. The Shannon limit on capacity is also shown, as are the upper bounds on the maximum achievable data rate for single carrier transmission using linear and decision feedback equalisers designed using the zero-forcing principle, as derived in Sec. 3.3. Note that the upper bound on the DFE performance is equal to the lower bound derived for the OFDM transmission (Sec. 3.2) when the number of subchannels used is the same. In the results presented here, the lower bound has been tightened by optimising the number of subchannels included in its calculation.

It can be seen from Fig. 5.2 that quantising the number of bits per sub-block reduces the overall OFDM performance by up to 2 dB at the lower SNRs, and by a much smaller amount at higher SNRs.

At low bit rates, the OFDM system gives an improved performance of as much as 6.5 dB over the linear equaliser and 4 dB over the upper bound of the DFE. At higher data rates, the improvement of OFDM over the linearly equalised single carrier reduces to 3 dB. The upper bound on the DFE approaches the OFDM performance at higher rates. It was shown in [33] that the lower bound, and hence the upper bound on DFE performance, becomes tighter as the SNR increases. In addition, at these higher SNRs, the error propagation effects of the DFE are reduced, and its performance approaches the upper bound.

This channel demonstrates the noise enhancing properties of the zero-forcing equaliser, which limit its use considerably. The overall gain-noise factor, k_{zf}, of the linear equaliser was found in (3.23)

$$k_{zf} = \left[\frac{1}{Z}\sum_{i=1}^{Z}\frac{1}{k_i}\right]^{-1} \tag{5.7}$$

The variation in k_i is about 15 dB, thus k_{zf} is dominated by the effects of the worst subchannels.

Figs. 5.3 and 5.4 show the optimum allocation of data among the subchannels at overall SNRs of 10 dB and 20 dB for an overall bit error probability of $p_e = 10^{-5}$. The optimisation was performed for both continuously variable and quantised data rates. It is seen that only the best 73 % of subchannels are used at 10 dB, whereas at 20 dB all but 3.2 % of the channel bandwidth is used.

The distributions of data which achieve capacity are also shown. The difference between the assignment for optimum OFDM and capacity is discussed in Sec. 7.

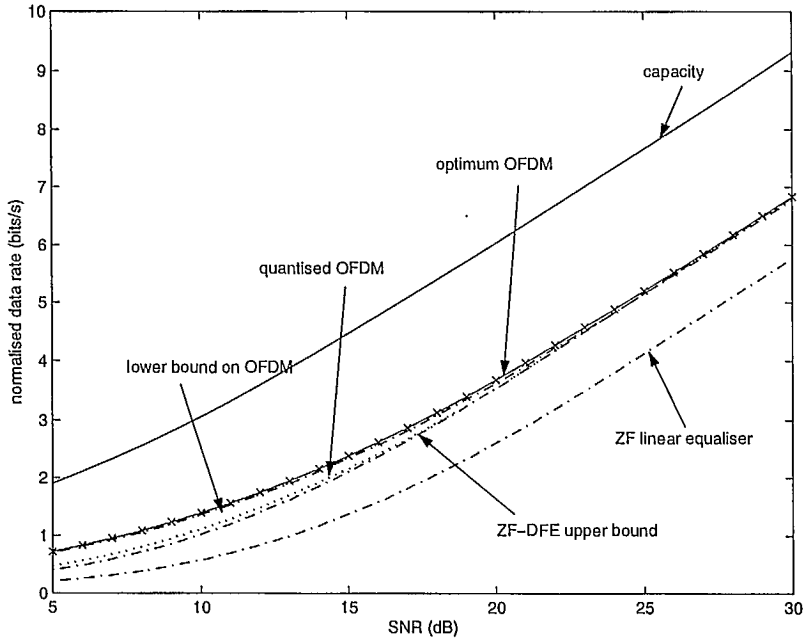

Figure 5.2: Data throughput for AWGN channel example for OFDM and equalised single carrier transmission, $Z = 256$, $p_e = 10^{-5}$.

The optimum power distributions at 10 dB and 20 dB are shown in Figs. 5.5 and 5.6. Note that the power scale is linear. In the continuously variable allocation of data, more power is concentrated in the subchannels with the best gain characteristics. The distribution for capacity is almost uniform over the bandwidth at higher SNRs. Using OFDM, the worst subchannels used are assigned only a fraction of the power for capacity. At higher SNRs, the best subchannels do receive an almost uniform power distribution, as was shown analytically in [33].

When the data allocation is quantised, this effect is overshadowed by the necessity to send only integer numbers of bits per sub-block. At 20 dB, the best subchannels transmitting at six bits per sub-block are allocated more power than the best of the subchannels transmitting at five bits. However, in order to transmit, for example, four bits on subchannels with worse gain characteristics, considerably more power is required. This is similar to the results found by Feig [12], although the performance in that system was suboptimal. The effects of this power allocation on the symbol and bit error probabilities can be seen in Figs. 5.7 and 5.8.

Figs. 5.7 and 5.8 shows the bit and symbol error probabilities across the subchannels for optimised continuously variable and quantised multicarrier transmission at overall SNRs of 10 dB and 20 dB, respectively. The bit and symbol error rate distributions are also shown in Figs. 5.9 and 5.10 vs. gain for SNRs of 5, 10, 20 and 30 dB. It is clear that the conditions stated by Kalet [17] and Bingham [4] of uniform bit or symbol error probabilities across are, at best, approximate with the approximation not holding well at low SNRs. At higher SNRs, the best subchannels do achieve fairly uniform symbol error probabilities, but this is not constant across the channel bandwidth.

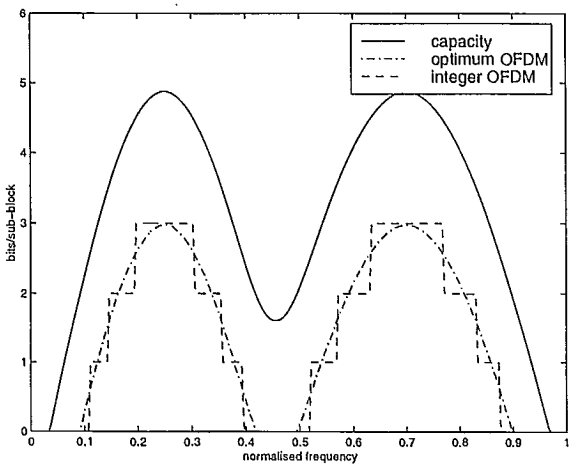

Figure 5.3: Optimum assignment of data at overall SNR 10 dB for $p_e = 10^{-5}$.

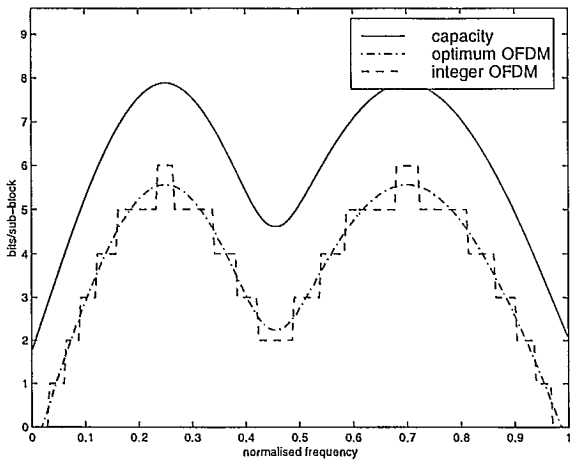

Figure 5.4: Optimum assignment of data at overall SNR 20 dB for $p_e = 10^{-5}$.

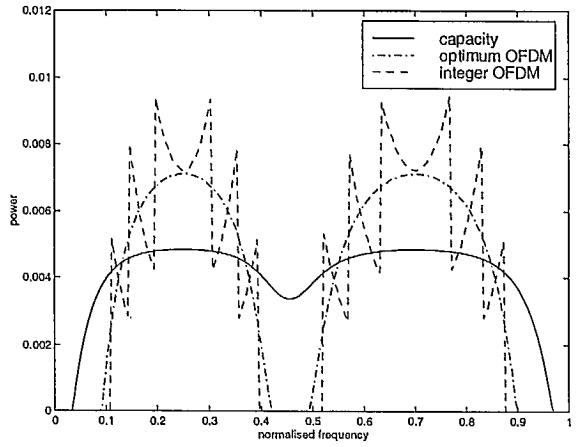

Figure 5.5: Optimum assignment of power at overall SNR 10 dB for $p_e = 10^{-5}$.

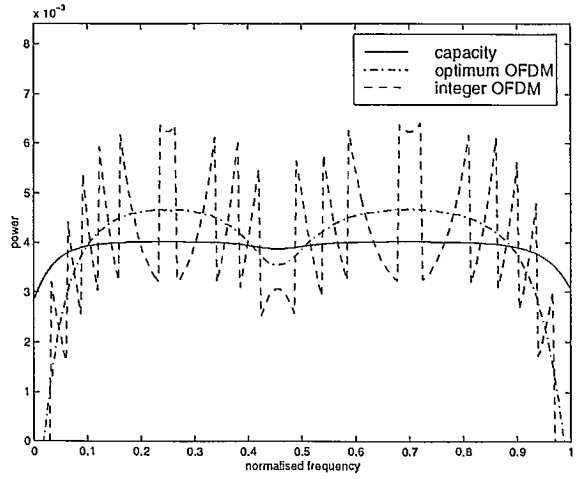

Figure 5.6: Optimum assignment of power at overall SNR 20 dB for $p_e = 10^{-5}$.

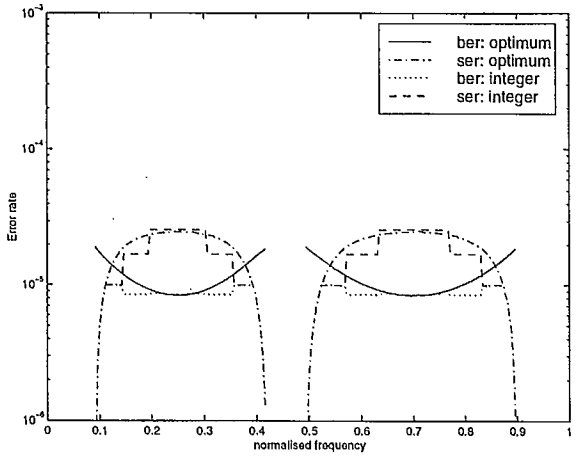

Figure 5.7: Error rates per bit and symbol at overall SNR 10 dB for $p_e = 10^{-5}$.

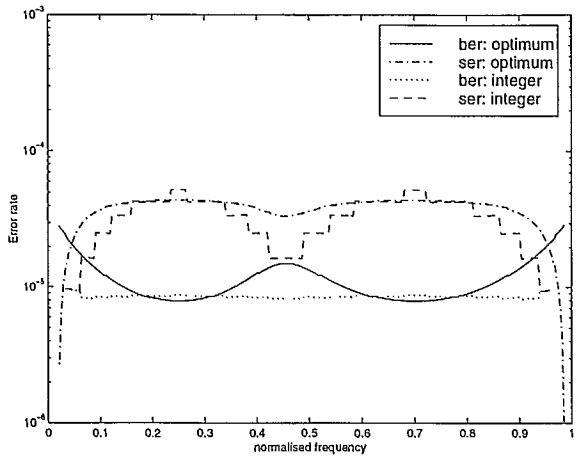

Figure 5.8: Error rates per bit and symbol at overall SNR 20 dB for $p_e = 10^{-5}$.

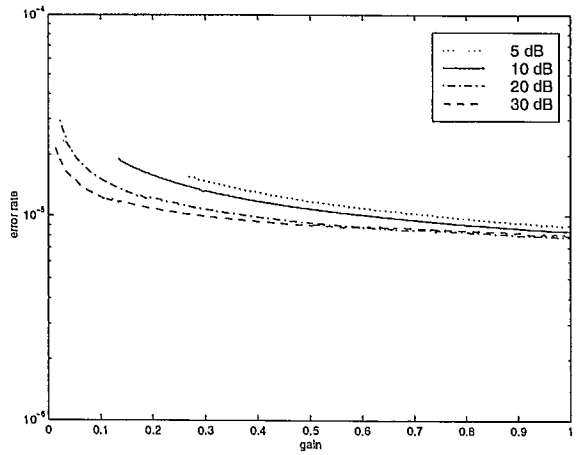

Figure 5.9: Distributions of bit error rate vs. gain for optimum OFDM at $p_e = 10^{-5}$.

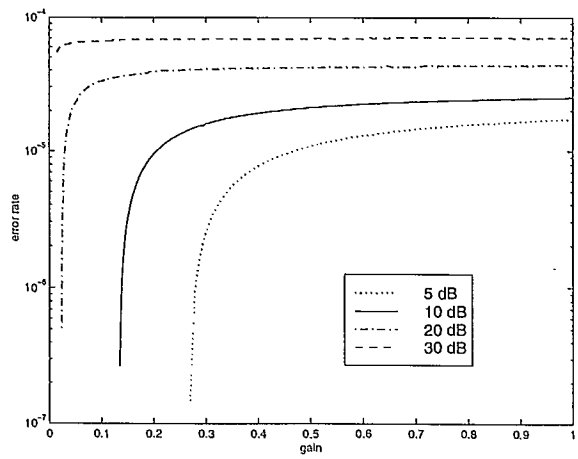

Figure 5.10: Distributions of symbol error rate vs. gain for optimum OFDM at $p_e = 10^{-5}$.

5.2 NMSE

The normalised mean-square error (NMSE) criterion was defined in Sec. 2.2.2 as

$$\epsilon = \frac{\sum_{i=1}^{Z} \frac{\sigma_i^2}{d_i^2}}{\sum_{i=1}^{Z} b_i} = \frac{\sum_{i=1}^{Z} \varepsilon_i}{R_b} \tag{5.8}$$

where the normalised mean-square error, ε_i, is the ratio of the mean-square error, σ_i^2, to the mean-square modulation distance, d_i^2. For QAM transmission, the normalised mean-square error is given by (Sec. 4.1)

$$\varepsilon_i = \frac{2(M_i - 1)}{3} \frac{1 + \frac{P_i k_i}{N_0 W_Z}}{\left(\frac{P_i k_i}{N_0 W_Z}\right)^2} \tag{5.9}$$

For optimum QAM transmission with no ISI or ICI, the constrained minimisation yields the gradient condition, (4.2),

$$\left.\frac{\partial \varepsilon_i}{\partial b_i}\right|_{\{b_i^*, P_i^*\}} = \zeta_1 \quad \text{and} \quad \left.\frac{\partial \varepsilon_i}{\partial P_i}\right|_{\{b_i^*, P_i^*\}} = \zeta_2 \tag{5.10}$$

This was solved using the algorithm presented in Sec. 2.3.1 for both continuously variable and quantised b_i's. The results are shown in Fig. 5.11 for an overall average normalised mean-square error $\epsilon = 0.05$. This value was chosen as the resulting achievable data rates are similar to those in the previous section using $p_e = 10^{-5}$. As for the error probability criterion, the reduction in achievable data rate using the quantised multicarrier is less than 1 dB. The lower bound on the maximum achievable data rate found in Sec. 4.2 is also shown. The bound has been tightened in this implementation by optimising the number of subchannels considered, which significantly improves its reliability, especially at at low SNRs where not all subchannels are used in the optimum allocation.

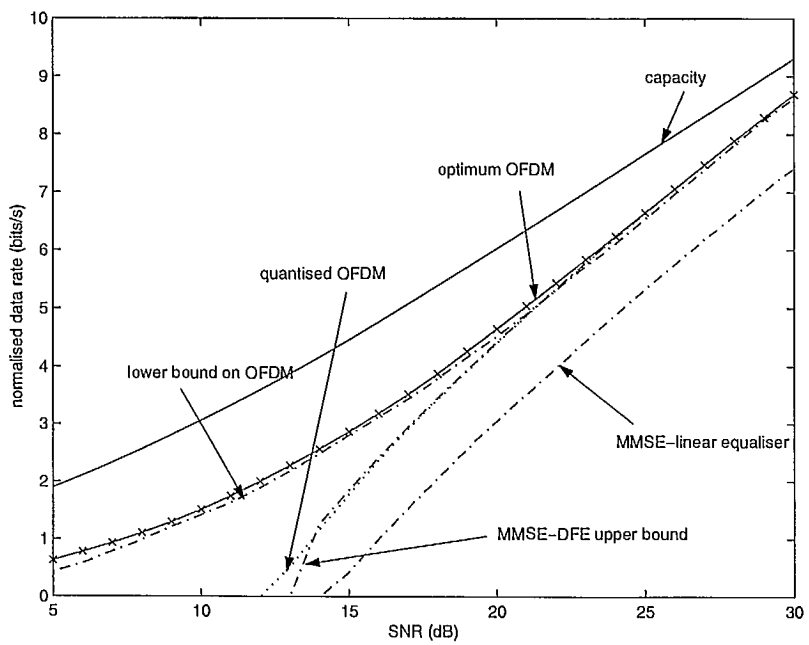

Figure 5.11: Data throughput for AWGN channel example for OFDM and equalised single carrier transmission, $Z = 256$, $\epsilon = 0.05$.

The data rate for the linear MMSE equaliser, the upper bound on decision feedback equalised single carrier transmission and the channel capacity are also shown in Fig. 5.11. At low SNRs, the multicarrier system shows a very significant improvement over both the equalised single carriers. At these SNRs, the assumption of error-free feedback sequences in the DFE is least valid. At higher SNRs, the upper bound on the data rate of the single carrier transmission using a DFE almost equals the multicarrier system. The multicarrier system shows an improvement of at least 4 dB over the linearly equalised single carrier at these higher SNRs.

The data distributions for an overall SNR of 10 and 20 dB are shown in Figs. 5.12 and 5.13. For the continuously variable and the quantised multicarrier, the minimum number of bits per sub-block is at least 2.6 and 2, respecitvely, and hence the convexity condition of Sec. 4.1 is met. Note that, at 10 dB, only 42 % of the subchannels are used, and at 20 dB, 86 % are assigned data.

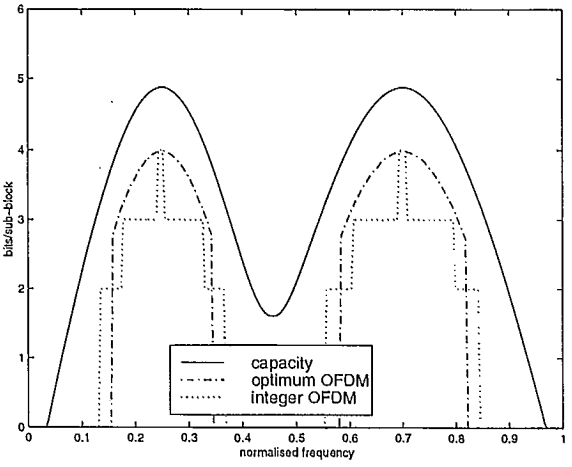

Figure 5.12: Optimum assignment of data at overall SNR 10 dB for $\epsilon = 0.05$.

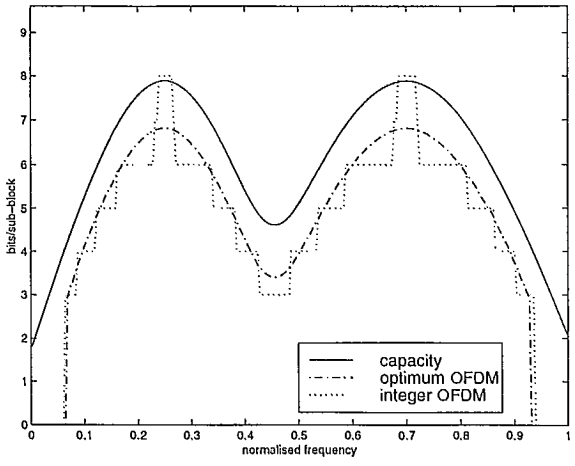

Figure 5.13: Optimum assignment of data at overall SNR 20 dB for $\epsilon = 0.05$.

The corresponding power distributions for these two cases are shown in Figs. 5.14 and 5.15, respectively. Note that the power scale is again linear. At the higher SNR, it appears that the power distribution follows the capacity distribution quite closely. In the quantised case, as with the error probability criterion, the power required to support the integer number of sub-blocks dominates the allocation pattern.

The relative NMSE per bit and per symbol on each subchannel is shown in Fig. 5.16 for 10 dB, and in Fig. 5.17 for 20 dB. Despite the inverse relationship of ε_i and P_i, (5.9), the NMSE per symbol has the same type of distribution as the power, i.e. the best subchannels have a higher value NMSE than the worst. The variation is less than 5% over the subchannels used. For the quantised multicarrier the variation is about 50% of the mean value. The NMSE per bit for the quantised case shows a fairly small deviation from that of the continuously variable data rate.

At high SNRs, P_i and ε_i tend to a uniform value across the subchannels used, as was shown analytically in [33].

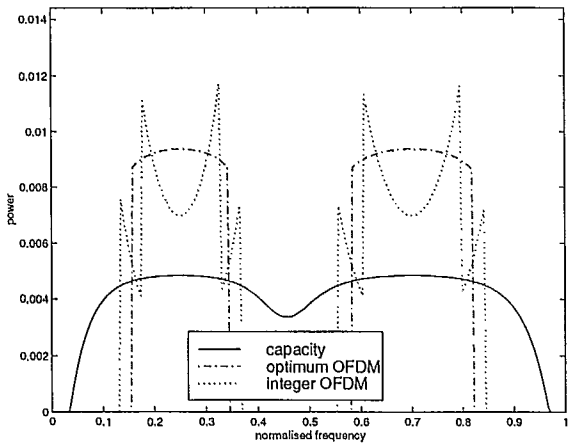

Figure 5.14: Optimum assignment of power at overall SNR 10 dB for $\epsilon = 0.05$.

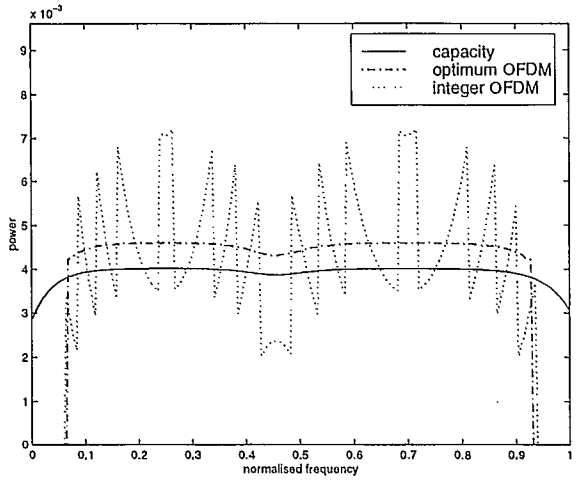

Figure 5.15: Optimum assignment of power at overall SNR 20 dB for $\epsilon = 0.05$.

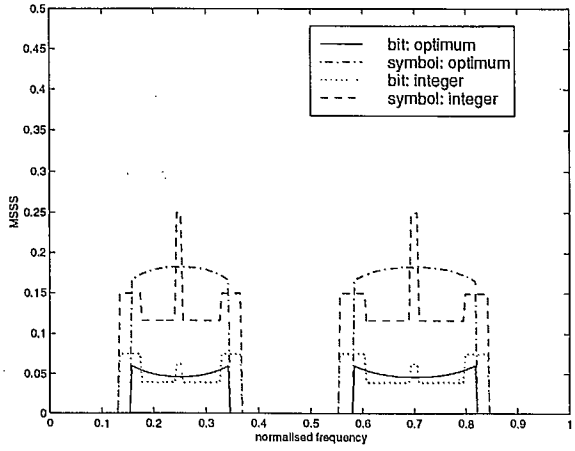

Figure 5.16: NMSE per bit and symbol (sub-block) for optimum OFDM at overall SNR 10 dB for $\epsilon = 0.05$.

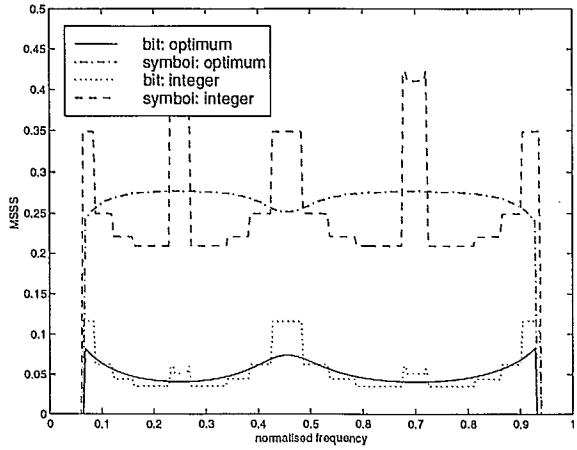

Figure 5.17: NMSE per bit and symbol (sub-block) for optimum OFDM at overall SNR 20 dB for $\epsilon = 0.05$.

6 MULTI-USER INTERFERENCE EXAMPLE

In this section, the effect of adjacent user interference on the optimum data and power assignments will be considered. The channel is Rayleigh fading, and the interference will be modelled, as a first approximation, as additive Gaussian noise, allowing the optimisation procedures presented previously to be applied.

6.1 SCENARIO

The scenario being considered is illustrated in Fig. 6.1. The channel is slow fading, and frequency selective over the individual multicarrier symbols. To mitigate the effects of ISI, a guard interval is used between sub-block transmissions. The user of interest is U_1 and the interference is due to timing differences between U_0 and U_1. Only optimisation of U_1 is considered; U_0 is assumed to be un-optimised. For ease of notation, it is also assumed that the subcarriers of U_0 have constant envelope signals.

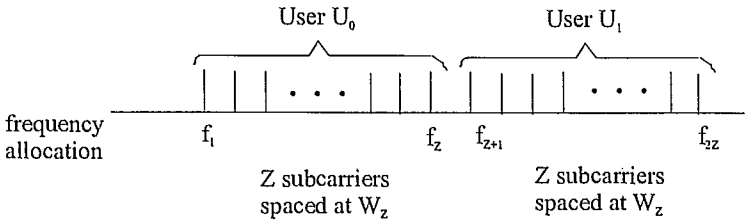

Figure 6.1: Multiuser multicarrier system

The subcarrier assignments are as follows:

$$\begin{aligned} U_0 &: f_i \quad i = 1, \ldots, Z \\ U_1 &: f_i \quad i = Z+1, \ldots, 2Z \end{aligned}$$

As the purpose of this example is to investigate the effects of the interference on the data and power assignments of U_1, it will be assumed that the channel gains and AWGN characteristics across the frequency band of U_1, i.e. k_i, $i = Z+1, \ldots, 2Z$, are constant over many symbol periods. Thus, without the interfering signal of U_0, the data and power assignments would be uniform across the subcarriers of U_1.

In the following section, the problem will be analysed in order to determine the level of interference experienced at each subcarrier of U_1, as a function of the time offset of the two users.

6.2 PROBLEM ANALYSIS

Consider a multicarrier system in which the symbol period is T, and the guard intervals between adjacent symbols is τ_g. On subchannel i with subcarrier frequency $f_i = w_i/2\pi$ and gain α_i, the allocated power is P_i and the data symbol in the time interval starting at mT is $b_i^{(m)}$. The group delay is τ on all subcarriers. At time t, user U_1 has the received signal

$$s_d(t) = \sum_{i=Z+1}^{2Z} \sum_{m=0}^{\infty} P_i b_i^{(m)} \alpha_i \, e^{j\, w_i (t - mT - \tau)} p(t - mT - \tau) \tag{6.1}$$

where $w_i = 2\pi f_i$, and α_i denotes the real channel gain. The time-gating function is

$$p(t) = \begin{cases} 1 & 0 \le t < T \\ 0 & \text{elsewhere} \end{cases} \tag{6.2}$$

Also define $T = T' + \tau_g$.

Note that the real channel gains, α_i, are assumed to be uncorrelated slow-fading Rayleigh-distributed random variables. For user U_1, it is assumed that the random gains on each subchannel are fixed for the duration of 'many' symbol periods. In frequency selective fading, these gains will not be identical across the subchannels. However, as the aim here is to demonstrate the effects of the interference on the optimal data and power assignments, for the purposes of this example the gains will be taken to be identical across the subchannels, $Z+1 \leq i \leq 2Z$. The assumption that these gains are fixed for many symbol periods permits the averaging of the effects of fading on the interfering user, U_0. In addition, it is assumed that each subchannel has fixed random phase. The phase is identified by the receiver and its effects are removed, and the use of timing recovery in the receiver allows the group delay τ to be set to zero.

It is assumed that the interfering user, U_0, has random gains and phases on each subchannel which are constant over the length of a single multicarrier symbol, and the relative delay between the interval periods of U_0 and U_1 is τ_I. The received interference from user U_0 is

$$s_I(t) = \sum_{i=1}^{Z} \sum_{m=0}^{\infty} B_i d_i^{(m)} \beta_i \, e^{j\, w_i (t - mT - \tau_I)} p(t - mT - \tau_I) \tag{6.3}$$

where, on subchannel i, $1 \leq i \leq Z$, with subcarrier frequency $f_i = w_i/2\pi$, B_i is the power allocation and the data symbols are $d_i^{(m)}$ in time interval m. The channel gains β_i are complex Gaussian random variables, uncorrelated over the different subcarrier frequencies.

For these two users, let the received signal be

$$r(t) = s_d(t) + s_I(t) + \eta(t) \tag{6.4}$$

and $\eta(t)$ is the additive Gaussian receiver noise with two-sided spectral density $\frac{N_0}{2}$.

6.2.1 Signal detection

At the U_1 receiver, the subcarrier at frequency f_i is correlated as

$$c_i^m = \int_{mT}^{(m+1)T} r(t)\, \phi_i(t - mT) dt \tag{6.5}$$

where the frequency function, $\phi_i(t)$, defined over an interval that takes into account the guard interval τ_g, is

$$\phi_i(t) = \begin{cases} e^{-j\, w_i\, t} & 0 \leq t \leq T' \\ 0 & \text{elsewhere} \end{cases} \tag{6.6}$$

Correlator output components due to the desired signal are free of interference due to the inherent orthogonality of the subcarriers, however components due to the interfering signal $s_I(t)$ are present.

The combined multiuser interference at subcarrier i, $Z+1 \leq i \leq 2Z$, at time interval m is computed from

$$\begin{aligned} c_i^m &= \int_{mT}^{mT+T'} (\text{ Interfering User } U_0 \text{ Rx Signal }) \, \phi_i(t - mT)\, dt \\ &= \int_{mT+\tau_I}^{mT+T'} \sum_{j=1}^{Z} \sum_{n=0}^{\infty} \beta_j B_j d_j^{(n)} e^{j w_j (t - nT - \tau_I)} p(t - nT - \tau_I) \phi_i(t - mT)\, dt \end{aligned} \tag{6.7}$$

and the noise component of the correlator output is

$$\int_{mT}^{mT+T'} \eta(t) \phi_i(t - mT)\, dt.$$

This interference signal has mean zero, assuming the constellations of the data symbols $d_i^{(n)}$ are symmetric about the real and imaginary axes, and that the symbols are equally probable. By the central limit theorem [23], the distribution of c_i^m may approache Gaussian if the number of significant terms in (6.7) is large. This has yet to be validated by simulation. The variance of the interfering signal amplitude on subchannel i is then given by

$$\sigma_{ci}^2 = \mathcal{E}\{c_i^m c_i^{m*}\} \tag{6.8}$$

where $\mathcal{E}\{\circ\}$ is the expected value. The independently faded channel gains β_j have cross-correlations zero, i.e. $\mathcal{E}\{\beta_j\,\beta_k^*\} = 0$ if $k \neq j$. As the signals on the interfering subcarriers are assumed to have constant envelope, the variance of the interfering power is

$$\sigma_{ci}^2 = \sum_{j=1}^{Z} \mathcal{E}\left\{\beta_j\,\beta_j^*\right\} B_j^2 \mathcal{E}\left\{\left|\sum_{n=0}^{\infty} \int_{mT+\tau_I}^{mT+T'} d_j^{(n)} e^{jw_j(t-nT-\tau_I)} p(t-nT-\tau_I)\phi_i(t-mT)\,dt\right|^2\right\}. \tag{6.9}$$

The interfering signals are assumed to be constant envelope, so $\mathcal{E}\{d_j^{(n)} d_k^{(m)*}\} = |d_j|^2 = \text{const}$. The guard interval is taken to be long enough to eliminate inter-symbol interference, hence terms with $n \neq m$ are dropped to yield

$$\sigma_{ci}^2 = \sum_{j=1}^{Z} \mathcal{E}\left\{\beta_j\,\beta_j^*\right\} B_j^2 |d_j|^2 \left|\int_{mT+\tau_I}^{mT+T'} e^{j[(w_j-w_i)(t-mT')-w_j\tau_I]}\,dt\right|^2. \tag{6.10}$$

Thus, writing $\sigma_{\beta_j}^2 = \mathcal{E}\left\{\beta_j\,\beta_j^*\right\}$, (6.10) becomes

$$\begin{aligned}
\sigma_{ci}^2 &= \sum_{j=1}^{Z} \sigma_{\beta_j}^2 B_j^2 |d_j|^2 \left|\int_{mT+\tau_I}^{mT+T'} \cos[(w_j-w_i)(t-mT)-w_j\tau_I]\,dt\right. \\
&\quad \left. + j\int_{mT+\tau_I}^{mT+T'} \sin[(w_j-w_i)(t-mT)-w_j\tau_I]\,dt\right|^2 \qquad (6.11) \\
&= \sum_{j=1}^{Z} \frac{\sigma_{\beta_j}^2 B_j^2 |d_j|^2}{(w_j-w_i)^2} \left|\sin[(w_j-w_i)T'-w_j\tau_I] + \sin(w_i\tau_I)\right. \\
&\quad \left. - j\left\{\cos[(w_j-w_i)T-w_j\tau_I] - \cos(w_i\tau_I)\right\}\right|^2. \qquad (6.12)
\end{aligned}$$

Define the real quantity of *interference gain* Γ_j^i, the interference observed on subchannel i due to the signal on subchannel j, as

$$\begin{aligned}
\Gamma_j^i &= \frac{1}{(w_j-w_i)^2} \left|\sin[(w_j-w_i)T'-w_j\tau_I] + \sin(w_i\tau_I)\right. \\
&\quad \left. + j\cos[(w_j-w_i)T'-w_j\tau_I] - \cos(w_i\tau_I)\right|^2. \qquad (6.13)
\end{aligned}$$

The effect of the interference on the correlator output variance due to all interferers is the sum of all Γ_j^i over $1 \leq j \leq Z$, and is shown in Fig. 6.2 as a function of adjacent-user delay τ_I. Numerical values for relative contributions to the total interference variance from individual interfering tones are given in Tables 6.1 and 6.2 for different adjacent channel interference delays. Note that the values given are normalised so that the total of interfering gains across the bandwidth of user U_1 is unity.

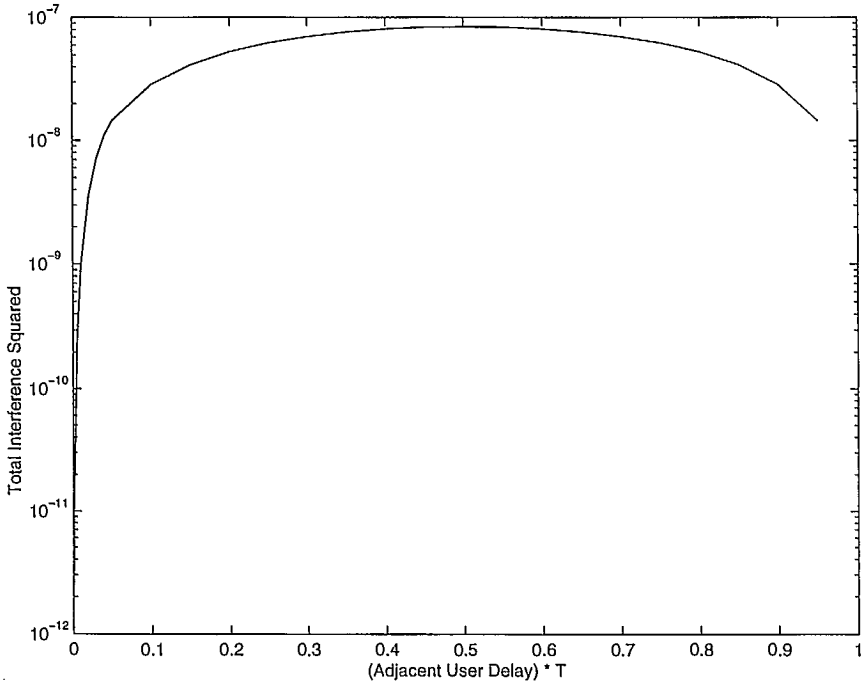

Figure 6.2: Total of interfering power versus adjacent user delay.

6.2.2 Statistics of interference terms

The correlator output corresponding to the interference signal at time interval m, c_i^m, has an approximately Gaussian distribution. The variance of the correlator output due to the interfering terms on subchannel i, $Z+1 \leq i \leq 2Z$, is

$$\sigma_{ci}^2 = \sum_{j=1}^{Z} \sigma_{\beta_j}^2 B_j^2 |d_j|^2 \Gamma_j^i \tag{6.14}$$

where $\sigma_{\beta_j}^2$ is the variance of the complex Gaussian random variable β_j, the gain of subchannel j, and the means are zero.

The interference will therefore be modelled as zero-mean Gaussian noise. The overall channel model is illustrated in Fig. 6.3.

For each subcarrier, the combined effects of the noise and interference can be modelled as additive Gaussian noise, hence the equivalent channel model is that shown in Fig. 6.4. This is clearly equivalent to the channel model used in Sec. 2.1, hence the optimisation procedures developed previously may be applied to this scenario.

6.3 EXAMPLE

For orthogonal signalling, i.e. the separation between subcarriers, $W_Z = f_{i+1} - f_i = 1/T_Z$, the amplitude of terms Γ_j^i are shown in Fig. 6.5 when $\tau_I = 0.2\,T_Z$ and $\tau_I = 0.5\,T_Z$.

The data and power assignments for user U_1 were optimised for an overall bit error rate of $p_e = 10^{-4}$. The SNR due to the AWGN is taken to be 30 dB for each of the following cases. Note that, as the AWGN has a flat power spectrum, i.e. $|H_N(f_i)|^2 = \text{const}$, the noise has no effect on the optimum resource allocation. It was seen in Tables 6.1 and 6.2 that 14 subchannels are significantly affected by interference from the adjacent user. In this example, only the first 20 subchannels of user U_1 are considered.

Table 6.1: Normalised total interference gains, $\sum_{j=1}^{Z} \Gamma_j^i$, on subcarrier i for $\tau_I = 0.1T$ to $0.5T$.

User U_1	τ_I/T				
Subcarrier i	0.1	0.2	0.3	0.4	0.5
Z+1	0.234127	0.456742	0.654103	0.785793	0.834692
Z+2	0.21177	0.298944	0.22599	0.0750386	1.1262e-11
Z+3	0.178305	0.132867	0.0106047	0.0333484	0.0927436
Z+4	0.138608	0.0285487	0.0215788	0.0491127	1.1262e-11
Z+5	0.0980762	4.56637e-11	0.0399755	1.68791e-11	0.0333877
Z+6	0.0616063	0.0126863	0.00959192	0.0218273	1.1262e-11
Z+7	0.0327531	0.0244031	0.00194718	0.00612597	0.0170345
Z+8	0.0132381	0.0186847	0.0141239	0.00468934	1.1262e-11
Z+9	0.00289163	0.0056397	0.00807594	0.00970142	0.0103048
Z+10	1.07186e-10	4.56637e-11	2.6429e-11	1.68791e-11	1.1262e-11
Z+11	0.00193414	0.00377412	0.0054054	0.00649397	0.00689828
Z+12	0.00588144	0.00830369	0.00627771	0.00208466	1.1262e-11
Z+13	0.00949463	0.00707601	0.000564925	0.00177574	0.00493901
Z+14	0.0113145	0.00233088	0.00176128	0.00400932	1.1262e-11

The optimum allocation of data for U_1 is shown in Fig. 6.6 for the relative delays $\tau_I = 0.2\,T_Z$ and $\tau_I = 0.5\,T_Z$ for an SIR of 10 dB. The data distribution is shown in Fig. 6.7 for the an SIR of 20 dB. The effect of the interference is clearly seen in the data distribution. Where the gain of the equivalent noise transfer function, $|H_E(f)|^2$, is very small, the subchannels have essentially no interference, hence the number of bits per sub-block is the same as on the un-interfered subchannels. On the other hand, where the interference is more marked the number of assigned bits is reduced. The difference among the subchannels is more marked at an SIR of 10 dB than at 20 dB, as the subchannel SIRs are lower.

The corresponding power distributions are plotted in Figs. 6.8 and 6.9. More power is assigned to the subchannels where the interference power is weak, and less where the subchannel SIR is low. At higher SIRs, the power assignment becomes more uniform.

The bit and symbol error rates corresponding to the optimum multicarrier conditions for user U_1 are shown in Figs. 6.10 and 6.11 for SIRs of 10 and 20 dB, respectively. The difference in ber is quite marked across the subchannels, varying from 10^{-4} to 4×10^{-4}, compared to the ser, which is more uniform. At the SIR increases, the ser becomes more uniform across the subchannels used.

Table 6.2: Normalised interference gains, $\sum_{j=1}^{Z} \Gamma_j^i$, on subcarrier i for $\tau_I = 0.6T$ to $0.9T$.

User U_1	τ_I/T			
Subcarrier i	0.6	0.7	0.8	0.9
Z+1	0.785795	0.654107	0.456747	0.234131
Z+2	0.0750354	0.225987	0.298944	0.211774
Z+3	0.0333504	0.0106032	0.132864	0.178306
Z+4	0.0491117	0.0215804	0.0285461	0.138607
Z+5	7.50181e-12	0.0399753	2.85396e-12	0.0980738
Z+6	0.0218278	0.00959071	0.0126877	0.061603
Z+7	0.00612509	0.00194779	0.0244037	0.0327498
Z+8	0.00469009	0.0141244	0.0186838	0.0132356
Z+9	0.00970099	0.00807513	0.00563863	0.00289038
Z+10	7.50181e-12	4.85428e-12	2.85396e-12	1.32325e-12
Z+11	0.0064943	0.00540601	0.00377492	0.00193506
Z+12	0.00208415	0.00627732	0.00830409	0.00588272
Z+13	0.0017762	0.00056459	0.00707551	0.00949571
Z+14	0.00400904	0.00176177	0.0023302	0.0113149

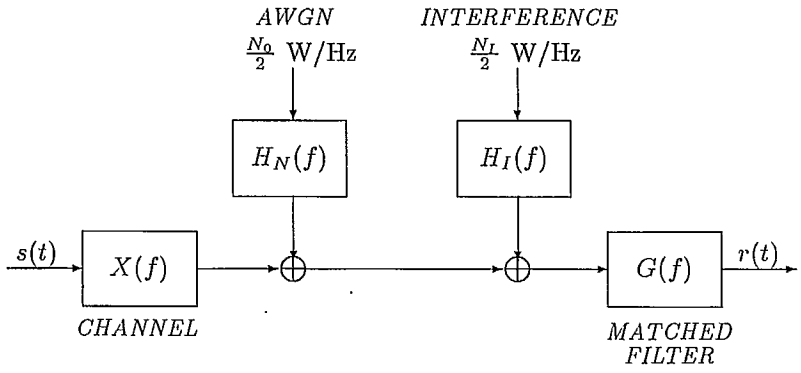

Figure 6.3: Interference model for multiuser multicarrier system

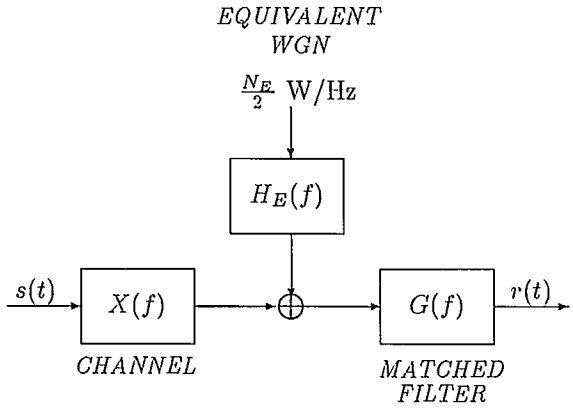

Figure 6.4: Equivalent channel model for multiuser multicarrier system

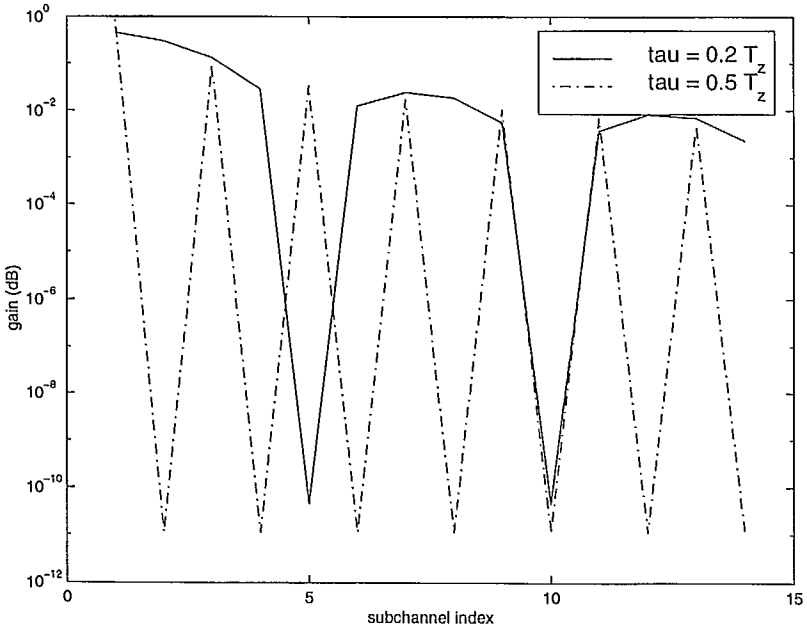

Figure 6.5: Relative gain of interference from adjacent user.

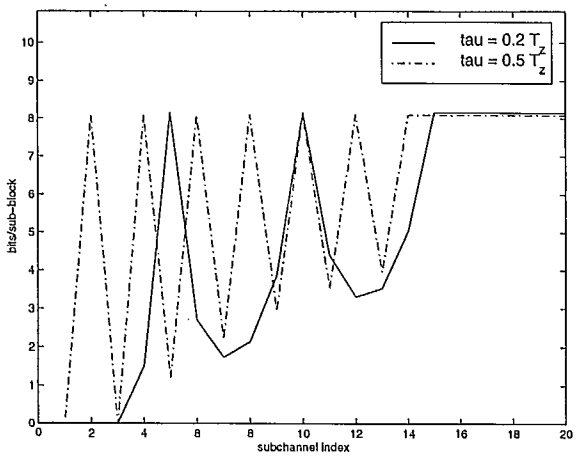

Figure 6.6: Optimum data distribution in the presence of multi-user interference at SIR 10 dB.

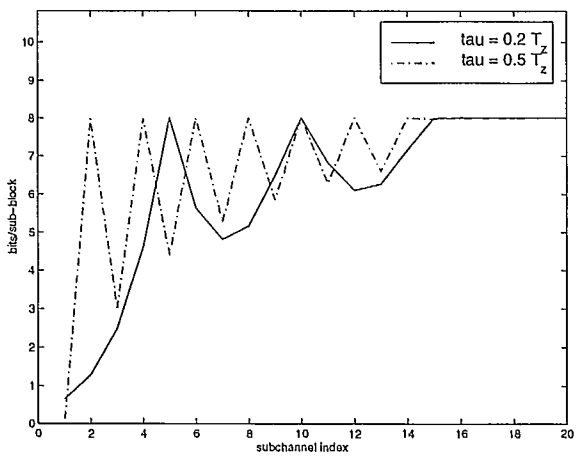

Figure 6.7: Optimum data distribution in the presence of multi-user interference at SIR 20 dB.

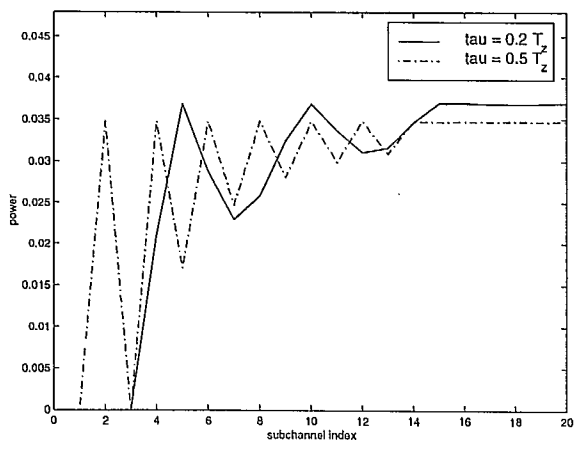

Figure 6.8: Optimum power distribution in the presence of multi-user interference at SIR 10 dB.

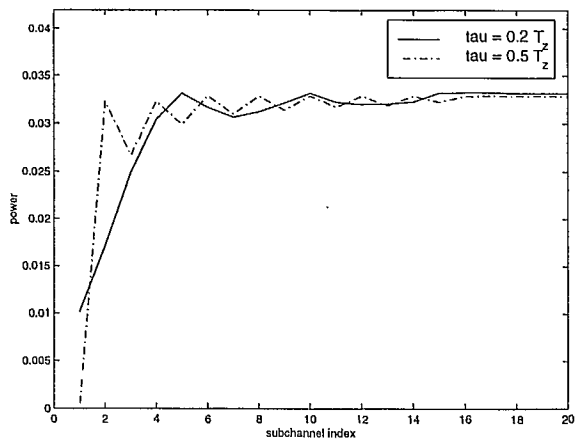

Figure 6.9: Optimum power distribution in the presence of multi-user interference at SIR 20 dB.

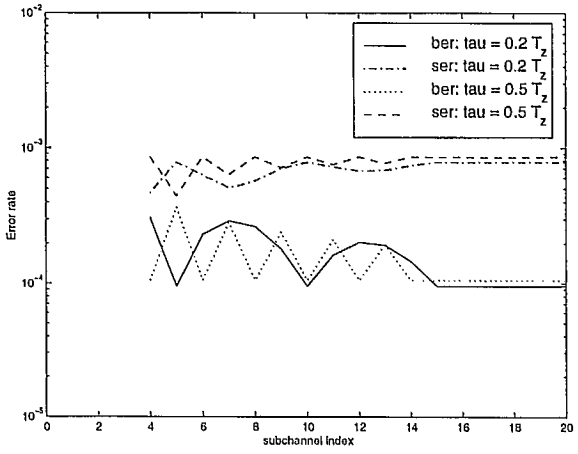

Figure 6.10: Bit and symbol error rate distributions for optimised multicarrier transmission in the presence of multi-user interference at SIR 10 dB.

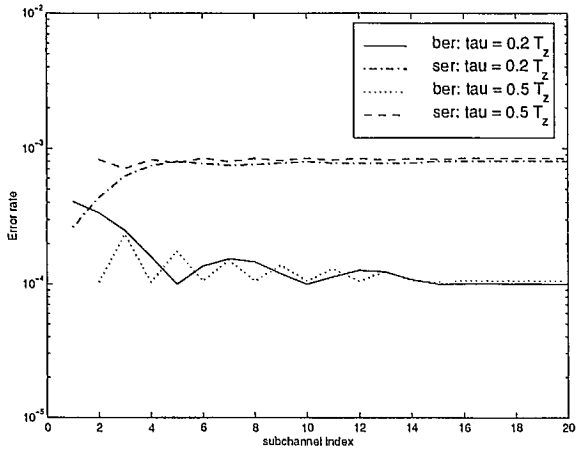

Figure 6.11: Bit and symbol error rate distributions for optimised multicarrier transmission in the presence of multi-user interference at SIR 20 dB.

7 NEARLY OPTIMAL ALLOCATIONS

The conditions for optimal allocation of data and power, presented in Sec. 2, can be satisfied only using an iterative approach. When the channel is varying, and the OFDM allocations must be adapted continuously, a more practical approach would trade-off the small increases in data rate obtained with the truly optimal solution against the speed with which a solution is found.

In this section, the results of the example of Sec. 5 will be examined to determine a nearly optimal approach to OFDM resource allocation. The optimisation criterion of interest here is the error probability, p_e. Recall that in the expression for symbol error probability on subchannel i, (3.9),

$$s_i = K_i erfc\left(\sqrt{\frac{3P_i k_i}{2N_0 W_Z (M_i - 1)}}\right) \tag{7.1}$$

the approximation $K_i = 2$ was made for the purposes of deriving a lower bound and comparing OFDM with single carrier equalised transmission in Sec. 2. In the implementation of the algorithmic solution used to generate the results in Sec. 5, this approximation was omitted, and the more precise term, $K_i = 2(1-1/\sqrt{M_i})$ was used.

Figs. 7.1 and 7.2 show the distributions of $M_i - 1$, where $M_i = 2^{b_i}$ is the number of data points per constellation, and received SNR, $\gamma_i = P_i k_i / N_0 W_Z$, plotted against the normalised channel gain-noise factors, k_i, for a range of overall SNRs. Both these distributions are very close to straight lines, where the nonlinearity in the slope is attributable to the $e^{-w_i^2}$ term in (3.11) and (3.12).

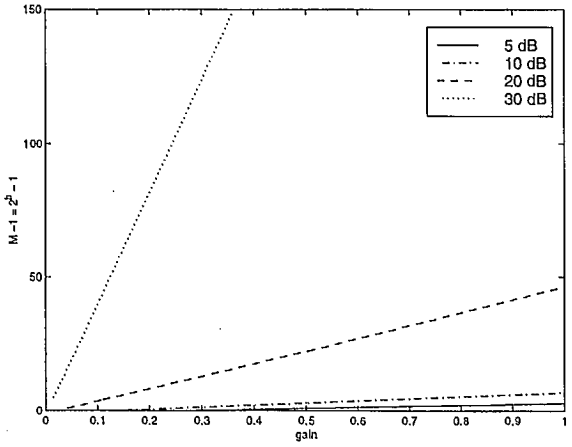

Figure 7.1: Distributions of number of points per constellation for optimum OFDM vs. channel gain (dashed lines).

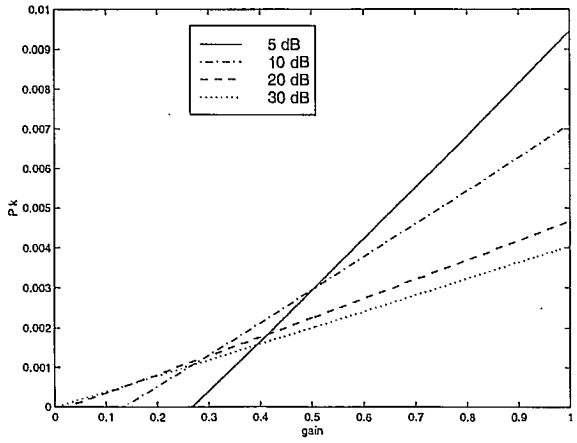

Figure 7.2: Distributions of received SNR for optimum OFDM vs. channel gain.

The values of $P_i k_i/(M_i - 1)$, plotted against the ordered gain-noise factors k_i, are shown in Fig. 7.3. It is seen that this factor is nearly constant across the whole range of k_i for which data and power are assigned.

From the section on capacity, Sec. 2.4, (2.35) gives the expression

$$\frac{P_i k_i}{C_i/W_Z - 1} = N_C W_Z \tag{7.2}$$

where C_i/W_Z is the capacity normalised by subchannel bandwidth, and $N_C/2$ is the two-sided power spectral density. Thus, a nearly optimal solution to the OFDM resource allocation would follow the distributions for capacity at a suitably modified noise level N_C.

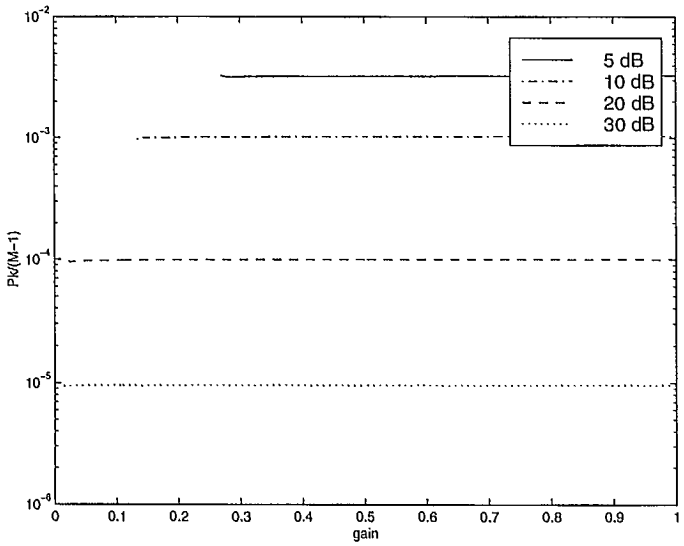

Figure 7.3: Distributions of $P_i k_i/(M_i - 1)$ for optimum OFDM vs. channel gain.

The aim is to find the value of the SNR $\gamma_C = P_{max}/NN_C W_Z$, where N is the number of subchannels used which gives the closest fit to optimal QAM-OFDM with an overall SNR of $\gamma_Q = P_{max}/ZN_0 W_Z$.

To find the equivalent noise, N_C, for the distribution using capacity, consider the relative bandwidth efficiencies of QAM and capacity, which are shown in Fig. 7.4 for a bit error probability of $p_e = 10^{-5}$, and SNR measured in bandwidth $W = ZW_Z$. For more detail on bandwidth efficiencies, see [26, chap. 5]. Note that here the bit error probability is considered, whereas in [26], the symbol error probability is used.

For the same bandwidth efficiency, the difference in SNRs between QAM and capacity is seen to be about 7.8 dB. This value can also be obtained by equating the terms $P_i k_i/(M_i - 1)$ from the QAM error probability and capacity expressions, (7.1) and (7.2) which yields

$$6N_0 W_Z \approx N_C W_Z \tag{7.3}$$

and $10 \log_{10} 6 = 7.8$dB.

The value of γ_C which gives the nearly optimal data and power distributions is then given by

$$10 \log_{10} \gamma_C = 10 \log_{10} \gamma_Q - 7.8 - 10 \log_{10} N/Z \tag{7.4}$$

Although the true value of N will not be known in advance of the solution, an estimate can be found, for example based on the number of subchannels used for achieving capacity distributions at an SNR of $10 \log_{10} \gamma_Q - 7.8$ dB.

7.1 AWGN EXAMPLE

In this section, the nearly-optimal allocation is applied to the example considered in Sec. 5. The channel characteristics are shown in Fig. 5.1, and the noise spectrum is uniform across the channel bandwidth. The number of subchannels used in the capacity allocations is shown in Fig. 7.5.

The aim is to find the nearly-optimal allocation for an overall SNR of 15 dB. From Fig. 7.5, at an SNR of $15 - 7.8 = 7.2$ dB, there are approximately $N = 227$ subchannels used of the $Z = 256$. Thus, from (7.4), the nearly-optimal OFDM allocation is obtained using the capacity allocation at $15 - 7.2 - 10 \log_{10} N/Z = 8.3$ dB.

Figs. 7.6 and 7.7 show the distributions of data for optimal OFDM and for the nearly-optimal OFDM described in this section. It is clear that the power allocations are very similar, while the number of bits

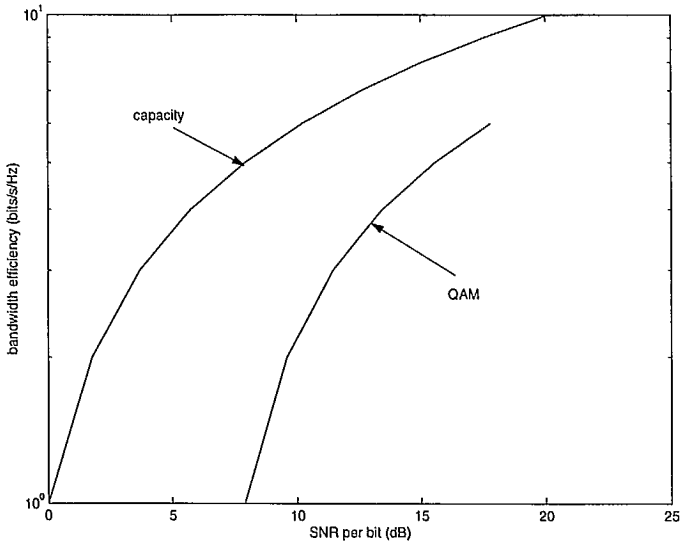

Figure 7.4: Bandwidth efficiencies for capacity and for QAM at $p_e = 10^{-5}$.

per sub-block is slightly lower on every subchannel for the nearly-optimal OFDM. Overall, the normalised throughput for the optimum OFDM is 2.38 bits/s, while for the nearly-optimal OFDM, it is 2.22 bits/s.

The "water-pouring" solution to OFDM power allocation was suggested in [4] and [28]. No details were given there regarding how to implement such an allocation, but it has been seen that the intuition was good, and that this water-pouring solution, when properly adjusted to account for SNR and the number of subchannels used, can provide a nearly-optimal OFDM solution for power allocation. The resulting data allocation also provides a distribution that is fairly close to that for OFDM.

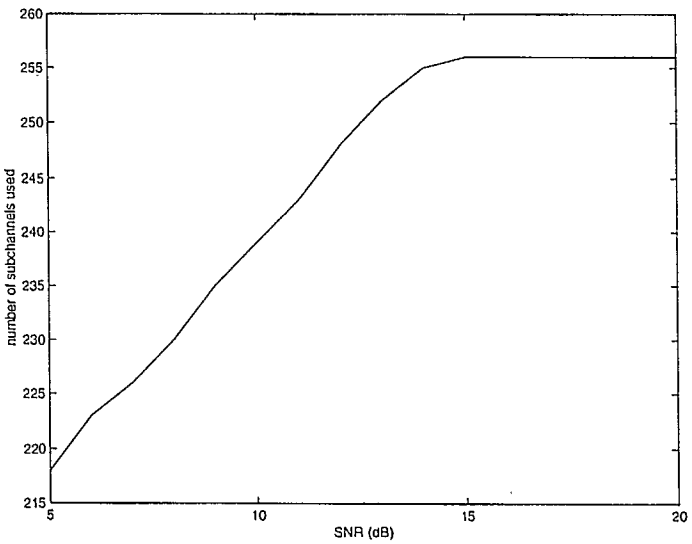

Figure 7.5: Number of subchannels used in capacity distributions for AWGN example.

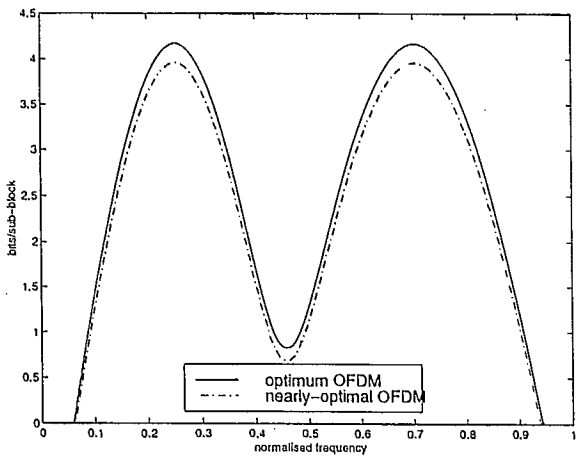

Figure 7.6: Distributions of data for optimal and nearly optimal OFDM at 15 dB, $p_e = 10^{-5}$.

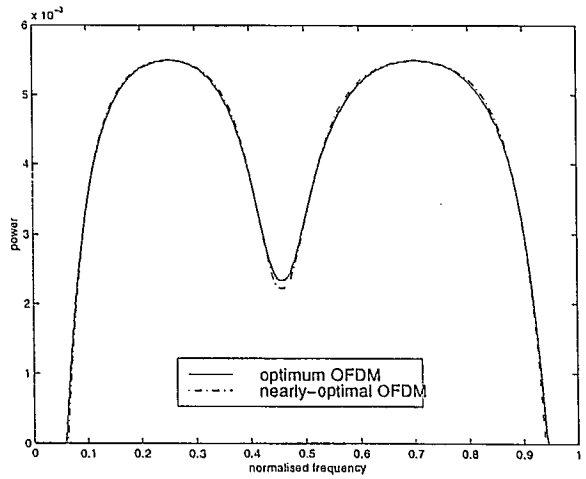

Figure 7.7: Distributions of power for optimal and nearly optimal OFDM at 15 dB, $p_e = 10^{-5}$.

8 CONCLUSIONS

The optimum conditions for maximising the data rate using OFDM transmission have been presented. It has been shown that these conditions are not met, in general, by subchannels achieving the same level of reliability as was previously assumed. An algorithm for achieving the conditions was presented and applied in two examples.

A lower bound on the transmission rate was found for the OFDM system which was identical to the upper bound found for the zero-forcing equalised single carrier transmission. It was therefore concluded that optimum OFDM transmission will achieve greater data rates than are possible using equalised single carrier transmission for all channels except one meeting the Nyquist I criterion. Using a notched channel with additive white Gaussian noise example transmitting orthogonally multiplexed QAM, it was seen that the largest gains over single carrier transmission are made at low and intermediate channel SNRs when not all subchannels are used for transmission. It is concluded that the assumption of uniform error probability across the subchannels results in only a small reduction in data throughput at high signal-to-noise ratios. However, at low and intermediate SNRs the optimum conditions found achieve a significantly higher data rate.

The distributions of the data and power across the channel bandwidth were examined and compared to the capacity distribution. In the optimised system, the subchannels with the best gain characteristics achieve the worst symbol error probabilities. This does not create a "weak link" effect, but in fact enhances the system performance. When the data rates on the subchannels are quantised, the overall performance is reduced by up to 1 dB. The distribution of power is changed significantly to assign more to the worst subchannels at each quantisation level, and these subchannels have the highest error probabilities.

The normalised mean-square error (NMSE) criterion was considered which enables a comparison to be made between OFDM transmission and single carrier transmission using equalisers designed using the minimum mean-square error principle. It was shown that OFDM transmission will always outperform a linear MMSE equaliser. The analytic comparison with a decision feedback equaliser was inconclusive, however it was demonstrated using the AWGN channel example that the multicarrier system does indeed outperform the single carrier using a DFE for a large range of SNRs.

The distributions of data and power across the subchannels were examined for the NMSE criterion. It was shown that for this criterion also, the optimum throughput was achieved when the subchannels with the best transmission characteristics have a worse than average normalised mean-square error.

The example of multi-user multicarrier transmission was considered, in which timing differences between adjacent users cause interference. This was modelled as additive Gaussian noise, and the effects of the interference on the optimal multicarrier distributions were considered. Further work is needed to validate the Gaussian noise model of interference.

A more practical approach to optimising the distributions of data and power was given in Sec. 7. It was seen that there are similar properties between the optimal OFDM allocation and the capacity distribution. Using the AWGN example of Sec. 5, it was seen that the "water-pouring" solution can be used to obtain a close approximation to the ideal allocation of power, while the data allocation is farther from optimum.

ACKNOWLEDGEMENTS

Parts of this Technical Note appeared in T. Willink's Ph.D. thesis and related publications. Other parts will appear in P. Vigneron's Ph.D. thesis.

This material will be presented at the 27th Annual Communications Theory Workshop, in Florida, USA, May 1998.

REFERENCES

[1] M. Abramowitz and I.A. Stegun, Eds., *Handbook of Mathematical Functions*, Dover, 1965.

[2] D.P. Bertsekas, *Constrained Optimization and Lagrange Multiplier Methods*, Academic Press, 1982.

[3] J.A.C. Bingham, *The Theory and Practice of Modem Design*, John Wiley & Sons, 1988.

[4] J.A.C. Bingham, "Multicarrier modulation for data transmission: An idea whose time has come", *IEEE Commun. Mag.*, pp. 5–14, May 1990.

[5] E.F. Casas and C. Leung, "OFDM for data communication over mobile radio FM channels — part I: Analysis and experimental results", *IEEE Trans. Commun.*, vol. 39, pp. 783–793, May 1991.

[6] R.W. Chang, "Synthesis of band-limited orthogonal signals for multichannel data transmission", *Bell Syst. Tech. J.*, vol. 45, pp. 1775–1796, Dec. 1966.

[7] R.W. Chang and R.A. Gibby, "A theoretical study of performance of an orthogonal multiplexing data transmission scheme", *IEEE Trans. Commun. Technol.*, vol. 16, pp. 529–540, Aug. 1968.

[8] J.S. Chow, J.C. Tu and J.M. Cioffi, "A discrete multitone transceiver system for HDSL applications", *IEEE J. Select. Areas Commun.*, vol. 9, pp. 895–908, Aug. 1991.

[9] P.S. Chow, J.C. Tu and J.M. Cioffi, "Performance evaluation of a multichannel transceiver system for ADSL and VHDSL services", *IEEE Select. Areas Commun.*, vol. 9, pp. 909–919, Aug. 1991.

[10] P.S. Chow, J.M. Cioffi and J.A.C. Bingham, "A practical discrete multitone transceiver loading algorithm for data transmission over spectrally shaped channels", *IEEE Trans. Commun.*, vol. COM-43, pp. 773–775, Apr. 1995.

[11] L.J. Cimini, "Analysis and simulation of a digital mobile channel using orthogonal frequency division multiplexing", *IEEE Trans. Commun.*, vol. 33, pp. 665–675, July 1985.

[12] E. Feig, "Practical aspects of DFT-based frequency division multiplexing for data transmission", *IEEE Trans. Commun.*, vol. 38, pp. 929–932, July 1990.

[13] R. Fortier, A. Ruiz and J.M. Cioffi, "Multidimensional signal sets through the shell construction for parallel channels", *IEEE Trans. Commun.*, vol. 40, pp. 500–512, Mar. 1992.

[14] R.G. Gallager, *Information Theory and Reliable Communications*, John Wiley & Sons, 1968.

[15] L.B. Glass, "Modern modem methods", *BYTE*, pp. 321–326, Jun. 1989.

[16] B. Hirosaki, S. Hasegawa and A. Sabato, "Advanced groupband data modem using orthogonally multiplexed QAM technique", *IEEE Trans. Commun.* vol. 34, pp. 587–592, June 1986.

[17] I. Kalet, "The multitone channel", *Proc. ICC*, pp. 1704–1710, 1987.

[18] I. Kalet, "The multitone channel", *IEEE Trans. Commun.*, vol. 37, pp. 119–124, Feb. 1989.

[19] S. Kasturia, J.T. Aslanis and J.M. Cioffi, "Vector coding for partial response channels", *IEEE Trans. Inform. Theory*, vol. 36, pp. 741–762, July 1990.

[20] B. Le Floch, R. Halbert-Lassalle and D. Castelain, "Digital sound broadcasting to mobile receivers", *IEEE Trans. Consum. Elect.*, vol. 35, pp. 493–503, Aug. 1989.

[21] D.G. Luenberger, *Introduction to Linear and Nonlinear Programming*, Addison-Wesley, 1973.

[22] Y. Nakamura, Y. Saito and S. Aikawa, "256 QAM modem for multicarrier 400 Mbit/s digital radio", *IEEE J. Select. Areas Commun.*, vol. 5, pp. 329–335, Apr. 1987.

[23] A. Papoulis, *Probability, random variables and stochastic processes*, McGraw-Hill, 1984.

[24] G.C. Porter, "Error distribution and diversity performance of a frequency-differential PSK HF modem", *IEEE Trans. Commun. Technol.*, vol. 16, pp. 567–575, Aug. 1968.

[25] R. Price, "Nonlinearly feedback-equalized PAM vs. capacity for noisy linear channels", *Proc. ICC*, 1972.

[26] J.G. Proakis, *Digital Communications*, McGraw-Hill, 1983.

[27] S.U.H. Qureshi, "Adaptive Equalization", *Proc. IEEE*, vol. 73, pp. 1349–1387, Sep. 1985.

[28] A. Ruiz and J.M. Cioffi, "A frequency domain approach to combined spectral shaping and coding", *Proc. ICC*, pp. 1711–1715, 1987.

[29] A. Ruiz, J.M. Cioffi and S. Kasturia, "Discrete multiple tone modulation with coset coding for the spectrally shaped channel", *IEEE Trans. Commun.*, vol. 40, pp. 1012–1029, June 1992.

[30] B.R. Saltzberg, "Performance of an efficient parallel data transmission system", *IEEE Trans. Commun. Tech.*, vol. 15, pp. 805–811, Dec. 1967.

[31] J. Salz, "Optimum mean-square decision feedback equalization", *Bell Syst. Tech. J.*, vol. 52, pp. 1341–1373, Oct. 1973.

[32] T.J. Willink and P.H. Wittke, "Comparison of optimised multicarrier and equalised single carrier transmission", *Proc. Cdn. Conf. Elec. and Comp. Eng.*, paper 30.1, Sep. 1993.

[33] T.J. Willink, "Multicarrier transmission and intersymbol interference in decision feedback equalisers", Ph.D. thesis, Dept. Elec. Eng., Queen's University, Ontario, Canada, Dec. 1993.

[34] T.J. Willink and P.H. Wittke "On optimizing multicarrier transmission", *Proc. International Symp. Info. Theory*, p. 397, Whistler, B.C., Canada, Sep. 17-22, 1995.

[35] T.J. Willink and P.H. Wittke "Optimization and performance evaluation of multicarrier transmission", *IEEE Trans. Info. Theory*, vol. 43, pp. 426–440, Mar. 1997.

[36] N.A. Zervos and I. Kalet, "Optimized decision feedback equalization versus optimized orthogonal frequency division multiplexing for high-speed data transmission over the local cable network", *Proc. ICC*, pp. 1080–1085, 1989.

[37] M.S. Zimmerman and A.L. Kirsch, "The AN/GSC-10 (KATHRYN) variable rate data modem for HF radio", *IEEE Trans. Commun. Technol.*, vol. 15, pp. 197–204, Apr. 1967.

[38] N.T. Zogakis and J.M. Cioffi, "The effect of timing jitter on the performance in a discrete multitone system", *IEEE Trans. Commun.* vol. COM-44, pp. 799–808, Jul. 1996.

A CONVEXITY CONDITIONS

In order for the constrained optimisation results to be applied, it must be confirmed that the criterion p_e or ϵ is convex with respect to b and P. The conditions for this to hold are derived in this appendix.

A.1 ERROR PROBABILITY CRITERION

For the Hessian to be positive semi-definite, it must be shown that $\frac{\partial^2 s_i}{\partial b_i^2}\frac{\partial^2 s_i}{\partial P_i^2} - \left[\frac{\partial^2 s_i}{\partial b_i \partial P_i}\right]^2 \geq 0$ for $i = 1, \ldots, N$. For the stationary point to be a minimum with respect to b_i and P_i, it is also necessary that $\frac{\partial^2 s_i}{\partial b_i^2} > 0$ and $\frac{\partial^2 s_i}{\partial P_i^2} > 0$.

Differentiating s_i with respect to P_i

$$\frac{\partial^2 s_i}{\partial P_i^2} = \frac{K_i}{\sqrt{\pi}} \frac{w_i e^{-w_i^2}}{P_i} \left[w_i^2 + \frac{1}{2}\right] \tag{A.1}$$

where $w_i^2 = \frac{3P_i k_i}{2N_0 W_Z (M_i - 1)}$. Also, differentiating s_i with respect to b_i, assuming that K_i is constant,

$$\frac{\partial^2 s_i}{\partial b_i^2} = \frac{K_i (\ln 2)^2}{\sqrt{\pi}} w_i e^{-w_i^2} \frac{M_i}{(M_i - 1)^2} \left[M_i w_i^2 - \frac{M_i}{2} - 1\right] \tag{A.2}$$

The second order derivative of s_i with respect to b_i and P_i is

$$\frac{\partial^2 s_i}{\partial b_i \partial P_i} = \frac{K_i}{\sqrt{\pi}} \frac{\ln 2}{2} \frac{M_i}{M_i - 1} \frac{w_i(1 - 2w_i^2)}{P_i} e^{-w_i^2} \tag{A.3}$$

After some manipulation, it is seen that

$$\frac{\partial^2 s_i}{\partial b_i^2}\frac{\partial^2 s_i}{\partial P_i^2} - \left[\frac{\partial^2 s_i}{\partial b_i \partial P_i}\right]^2 = \frac{K_i^2}{\pi} \left[\frac{w_i e^{-w_i^2} \ln 2}{P_i (M_i - 1)}\right]^2 \left[M_i^2 (w_i^2 - \frac{1}{2}) - M_i (w_i^2 + \frac{1}{2})\right] \tag{A.4}$$

Hence the Hessian is positive semi-definite if

$$M_i (w_i^2 - \frac{1}{2}) \geq (w_i^2 + \frac{1}{2}) \tag{A.5}$$

For example, if the symbol error probability on the ith subchannel is $s_i \leq 10^{-4}$, then $w_i \geq 2.75$ and a sufficient condition for convexity is $M_i > 1.14$ or $b_i > 0.19$.

For the solution to be a minimum, it is necessary that $\frac{\partial^2 s_i}{\partial P_i^2} > 0$ and $\frac{\partial^2 s_i}{\partial b_i^2} > 0$. For the first condition, it is seen from (A.1) that s_i is convex with respect to P_i if

$$w_i^2 + \frac{1}{2} > 0 \tag{A.6}$$

which holds for all real values of $w_i > 0$.

Similarly, from (A.2), the stationary point is a minimum with respect to b_i if

$$\frac{3P_i k_i}{2N_0 W_Z} \frac{M_i}{M_i - 1} - \frac{M_i}{2} - 1 > 0 \tag{A.7}$$

As $\frac{M_i}{M_i - 1} > 1$, a sufficient condition for $M_i = 2^{b_i}$ to satisfy this condition is

$$\frac{M_i}{2} \leq \frac{3P_i k_i}{2N_0 W_Z} - 1 \tag{A.8}$$

If $\frac{P_i k_i}{N_0 W_Z} > 1$, i.e. the received SNR on the ith subchannel, $\gamma_{r,i}$, is greater than 0 dB, then for convexity, the parameter w_i is bounded by

$$w_i^2 \geq \frac{3P_i k_i}{2N_0 W_Z \left(\frac{3P_i k_i}{N_0 W_Z} - 3\right)} > \frac{1}{2} \tag{A.9}$$

A.2 NMSE CRITERION

Since R_b and the constraint function h_1 given by (2.9) are linear with respect to the minimisation parameters, $\boldsymbol{b}$ and $\boldsymbol{P}$, the Lagrangian function is convex if and only if the second constraint function h_2

$$h_2 = \frac{\sum_{i=1}^{Z} \varepsilon_i}{R_b} - \epsilon_{max} = 0 \tag{A.10}$$

is convex. This requirement is satisfied if $\frac{\partial^2 \varepsilon_i}{\partial b_i^2}\frac{\partial^2 \varepsilon_i}{\partial P_i^2} - \left[\frac{\partial^2 \varepsilon_i}{\partial b_i \partial P_i}\right]^2 \geq 0$ and if the second order derivatives satisfy $\frac{\partial^2 \varepsilon_i}{\partial b_i^2} > 0$ and $\frac{\partial^2 \varepsilon_i}{\partial P_i^2} > 0$ for $i = 1, \ldots, N$.

Differentiating h_2 with respect to P_i

$$\frac{\partial^2 \varepsilon_i}{\partial P_i^2} = \frac{1}{R_b}\frac{2(M_i - 1)}{3}\frac{N_0 W_Z}{k_i}\left(\frac{2}{P_i^3} + \frac{N_0 W_Z}{k_i}\frac{6}{P_i^4}\right) \tag{A.11}$$

Differentiating with respect to b_i

$$\frac{\partial^2 \varepsilon_i}{\partial b_i^2} = \frac{2N_0 W_Z}{3P_i k_i}\left[1 + \frac{N_0 W_Z}{P_i k_i}\right]\frac{M_i(R_b \ln 2 - 1)^2 + M_i - 2}{R_b^3} \tag{A.12}$$

The second order derivative with respect to b_i and P_i is

$$\frac{\partial^2 \varepsilon_i}{\partial b_i \partial P_i} = -\frac{2}{3}\frac{N_0 W_Z}{P_i k_i}\left[\frac{R_b M_i \ln 2 - M_i + 1}{R_b^2}\right]\left[\frac{1}{P_i} + 2\frac{N_0 W_Z}{P_i^2 k_i}\right] \tag{A.13}$$

After some manipulation, the Hessian is given by

$$\begin{aligned}\frac{\partial^2 \varepsilon_i}{\partial b_i^2}\frac{\partial^2 \varepsilon_i}{\partial P_i^2} - \left[\frac{\partial^2 \varepsilon_i}{\partial b_i \partial P_i}\right]^2 = \frac{4}{9R_b^4 P_i^2}\left(\frac{N_0 W_Z}{P_i k_i}\right)^2 \Bigg\{ \left(1 + 4\frac{N_0 W_Z}{P_i k_i}\right) \cdot \\ \left[(M_i^2 - M_i)(R_b \ln 2 - 1)^2 + (2M_i - 3)(M_i - 1) - M_i R_b^2 (\ln 2)^2\right] \\ + \left(\frac{N_0 W_Z}{P_i k_i}\right)^2 \left[2(M_i^2 - M_i)(R_b \ln 2 - 1)^2 + 2(M_i - 1)(3M_i - 4) - 2M_i R_b^2 (\ln 2)^2\right] \Bigg\}\end{aligned} \tag{A.14}$$

Thus it can be seen that the Hessian is positive semi-definite at least for all $M_i \geq 3$, i.e. for all $b_i \geq 1.6$. From (A.11) and (A.12), all values of M_i satisfying this condition also satisfy $\frac{\partial^2 \varepsilon_i}{\partial P_i^2} > 0$ and $\frac{\partial^2 \varepsilon_i}{\partial b_i^2} > 0$.